

Supporting Information

The mechanism of Fe induced bond stability of uranyl(V)

T. Vitova,^{1*} R. Faizova,² J. I. Amaro Estrada,³ L. Maron,^{3*} T. Pruessmann,¹ T. Neill,¹ A. Beck,¹ B. Schacherl,¹ F. Fadaei-Tirani,² M. Mazzanti^{2*}

¹Karlsruhe Institute of Technology (KIT), Institute for Nuclear Waste Disposal (INE), P.O. 3640, D-76021 Karlsruhe, Germany.

²Institut des Sciences et Ingénierie Chimiques, Ecole Polytechnique Fédérale de Lausanne (EPFL), 1015 Lausanne, Switzerland

³LPCNO, University of Toulouse, INSA Toulouse 135, avenue de Rangueil, Toulouse cedex 31077, France

Table of Contents

EXPERIMENTAL DETAILS.....	4
1. GENERAL CONSIDERATIONS.....	7
2. EXPERIMENTAL PROCEDURES	8
SYNTHESIS OF COORDINATION COMPLEXES OF MESALDIEN ²⁻ LIGAND.....	8
SYNTHESIS OF [Fe(TPA)(Py)U ^V O ₂ (MESALDIEN)]I (3).....	9
SYNTHESIS OF [Ui ₂ (MESALDIEN)] (5).....	9
SYNTHESIS OF COORDINATION COMPLEXES OF DPAEA ²⁻ LIGAND.....	10
3. NMR SPECTRA	11
FIGURE S1. ¹ H NMR (400MHz, C ₅ D ₅ N, 298K) OF COMPLEX [Fe(TPA)(Py)U ^V O ₂ (MESALDIEN)]I (3).....	11
FIGURE S2. ¹ H NMR (400MHz, C ₅ D ₅ N, 298K) OF COMPLEX [Ui ₂ (MESALDIEN)] (5).....	12
4. CRYSTALLOGRAPHIC DATA.....	13
FIGURE S3. ELLIPSOID PLOT AT 50% PROBABILITY OF X-RAY MOLECULAR STRUCTURES OF COMPLEXES 1-8.....	15
FIGURE S4. ELLIPSOID PLOT AT 50 % PROBABILITY OF COMPLEX 3.....	16
FIGURE S5. ELLIPSOID PLOT AT 50 % PROBABILITY OF COMPLEX 5.....	17
TABLE S1. CRYSTALLOGRAPHIC DATA OF 3 AND 5.....	18
5. MOLECULAR STRUCTURES DESCRIPTION	19
TABLE S2. COMPARISON OF BOND LENGTHS IN COMPLEXES 1 AND 6.....	22
TABLE S3. COMPARISON OF BOND LENGTHS IN COMPLEXES 2 AND 7.....	22
TABLE S4. COMPARISON OF BOND LENGTHS IN COMPLEXES 2, 3 AND 4.	23
TABLE S5. COMPARISON OF BOND LENGTHS IN COMPLEXES 1 AND 5.....	23
6. COMPUTATIONAL DETAILS	24

FIGURE S9. DFT-BASED NBO ANALYSIS FOR COMPLEX 6	29
FIGURE S10. CASSCF COMPUTED ENERGY SPECTRUM AND DEPICTION OF THE CHOOSES ACTIVE ORBITALS FOR COMPLEX 7	30
FIGURE S11. NPA CHARGES FOR COMPLEX 7.....	31
FIGURE S12. DFT COMPUTED ENERGY SPECTRUM FOR COMPLEX 7.....	32
FIGURE S15. NPA CHARGES FOR COMPLEX 1.....	35
FIGURE S16. DFT COMPUTED ENERGY SPECTRUM FOR COMPLEX 1.....	36
.....	38
FIGURE S17. DFT-BASED NBO ANALYSIS FOR COMPLEX 1	38
FIGURE S20. DFT COMPUTED ENERGY SPECTRUM FOR COMPLEX 2.....	41
FIGURE S21. DFT-BASED NBO ANALYSIS FOR COMPLEX 2	45
FIGURE S25. DFT-BASED NBO ANALYSIS FOR COMPLEX 3	49
TABLE S6. CARTESIAN COORDINATES OF ALL OPTIMIZED STRUCTURES.....	50
 7. X-RAY ABSORPTION SPECTROSCOPY	57
U L₃ EDGE XANES AND EXAFS OF COMPLEXES 1 – 3.....	57
FIGURE S27. UL₃ EDGE EXAFS (LEFT) AND FOURIER TRANSFORMED EXAFS (RIGHT) OF COMPLEXES 1, 2 AND 3 WITH FITS (DASHED BLACK LINES).	58
TABLE S7. EXAFS FITTING PARAMETERS AND BOND LENGTHS FROM CRYSTALLOGRAPHIC DATA (CRY)	58
U M_{4,5} EDGE HR-XANES EXPERIMENTS AND FDMNES COMPUTATIONS.....	60
FIGURE S28. U M₄ EDGE HR-XANES (POST EDGE REGION) OF COMPOUNDS 1 – 8.	60
FIGURE S30. U M₄ EDGE HR-XANES OF COMPOUNDS 1 – 3 AND SPECTRA OF THE DIFFERENT U SITES CALCULATED BY FDMNES.	61
FIGURE S31. OCCUPIED U P, D, F – DOS, O P – DOS AND N P – DOS AS WELL AS XES SPECTRA CONSIDERING THE SELECTION RULES FOR THE U M₄ AND U M₅ ABSORPTION EDGES.	62
FIGURE S32. OCCUPIED U P, D, F – DOS, O P – DOS AND N P – DOS AS WELL AS HR-XANES SPECTRA CONSIDERING THE SELECTION RULES FOR THE U M₄ AND U M₅ ABSORPTION EDGES.	63
EXAMPLE FDMNES INPUT FILE	64
 REFERENCES.....	65

EXPERIMENTAL DETAILS

Syntheses and characterisation of the 1-8 compounds. All manipulations were performed in Ar glove box, using dried and degassed solvents and reagents. Complexes $[U^{VI}O_2(\text{Mesaldien})]I$ (**1**), $\{[U^{VI}O_2(\text{Mesaldien})]K\}_n$ (**2**),^[1] $\{\text{Fe}(TPA)\text{Cl}\}\{UO_2(\text{Mesaldien})\}\{\text{Fe}(TPA)\text{Cl}\}I$ (**4**),^[2] $[U^{VI}O_2(\text{dpaea})]$ (**6**), $[\text{K}(2.2.2.\text{cryptand})][U^{VI}O_2(\text{dpaea})]$ (**7**), $[U^{IV}(\text{dpaea})_2]$ (**8**)^[3] were prepared according to previously published procedures (cf. Figure 1). The novel compounds $[\text{Fe}(TPA)(\text{Py})U^{VI}O_2(\text{Mesaldien})]I$ (**3**) and $[\text{UI}_2(\text{Mesaldien})]$ (**5**) have been prepared and characterized by single crystal X-ray diffraction, proton NMR and elemental analysis (cf. Figure 1 and SI for detailed description).

Synthesis of $[\text{Fe}(TPA)(\text{Py})U^{VI}O_2(\text{Mesaldien})]I$ (3**).** An orange suspension of $[\text{Fe}(TPA)]_2$ prepared *in situ* from the reaction of FeI_2 (11.1 mg, 0.036 mmol, 1 equiv.) with TPA (10.5 mg, 0.036 mmol, 1 equiv.) in 1 mL of pyridine is added to a stirred dark blue solution of $\{[U^{VI}O_2(\text{Mesaldien})]K\}_n$ prepared *in situ* from the reaction of $[(UO_2\text{Py}_5)(\text{KI}_2\text{Py}_2)]_n$ (40.0 mg, 0.036 mmol, 1 equiv.) with $\text{K}_2\text{Mesaldien}$ (14.4 mg, 0.036 mmol, 1 equiv.) in 2 mL of pyridine. Immediately the resulting solution changes colour to dark red. The reaction mixture was stirred overnight. The resulting solution was filtered and X-ray quality crystals of $[\text{Fe}(TPA)(\text{Py})UO_2(\text{Mesaldien})]I$ (26.5 mg, 0.022 mmol, 60%) were obtained by slow diffusion of hexane. Elemental analysis calcd (%) for $[\text{Fe}(TPA)(\text{Py})UO_2(\text{Mesaldien})]I.(KI)_1$ ($C_{37}H_{39}I_2N_7O_4FeK_1U$ MW=1232.545) 36.06; H, 3.19; N, 7.95. Found: C, 35.84; H, 2.78; N, 7.63. **Synthesis of $[\text{UI}_2(\text{Mesaldien})]$ (**5**).** A solution of 43.6 mg of $[\text{UI}_4(\text{dioxane})_{1.8}]$ (0.05 mmol, 1 equiv.) in pyridine (1.5 mL) was added to a suspension of 19.4 mg of $\text{K}_2\text{Mesaldien}$ (0.05 mmol, 1 equiv.) in 1.5 mL of pyridine yielding after 15 minutes a dark red solution, that was filtered and set for crystallization. 31 mg (0.036, 72%) of dark red crystals suitable for X-Ray of $[\text{UI}_2(\text{Mesaldien})]$ were collected after slow diffusion of 1,4-dioxane or DIPE. ^1H NMR (200 MHz, C_5D_5N , 298 K): δ = 96.34 (s, 2H), 43.26 (s, 2H), 30.80 (s, 2H), 24.36 (d, 4H), 17.96 (s, 2H), 15.46 (s, 2H), -2.08 (s, 3H), -26.54 (s, 2H), -37.76 (s, 2H). Elemental analysis (%) calcd for $[\text{UI}_2(\text{Mesaldien})].0.17\text{KI}$ $C_{19}H_{21}I_2N_3O_2U(KI)_{0.17}$: C, 27.06; H, 2.51; N, 4.98. Found: C, 26.65; H, 2.92; N, 5.10.

HR-XANES and VB-RIXS experiments and computations. The U M_4 (3726 eV) and M_5 (3550 eV) edge HR-XANES and VB-RIXS spectra of complexes **1-8** were measured using the Johann type X-ray emission spectrometer installed at the CAT-ACT beamline, ACT experimental hutch for actinide research at the KIT Light Source, Karlsruhe, Germany.^[4] The incident energy was monochromatized by a Si(111) double crystal monochromator (DCM). Sample, analyzer crystals and a single diode VITUS silicon drift detector (VITUS SDD KETEK) were arranged in a vertical Rowland geometry. A glove box encompassing the spectrometer and maintaining constant He flow was installed to avoid intensity losses due to scattering and absorption of photons. The HR-XANES spectra were obtained by recording the maximum intensity of the M_α (M_5N_7 , 3171.0 eV)/ M_β (M_4N_6 , 3337.0 eV) emitted fluorescence diffracted by one (Figure 3)/four (Figure 6) spherically bent Si(220) (M_4)/Ge(220) (M_5 edge) crystal analyzers (SAINT-GOBAIN) with 1m bending radius and focused onto the detector. The energy resolution of the U M_4 edge HR-XANES spectra was improved when one crystal was used (Figure 3). The crystals were aligned at 77.8° (M_5, M_α) or 75.36° (M_4, M_β) Bragg angles. Details on the U L_3 edge XANES and extended X-ray absorption near edge structure (EXAFS) measurements and analyses of the spectra of complexes **1**, **2** and **3** are given in SI (cf. Figures S26, S27,

Table S7). The energy positions of the first inflection points of the rising absorption edges of the spectra of **1**, **2** and **3** were compared. Those correspond to the energy positions of the maxima of the first intensive peaks of the first derivative spectra. The uncertainty in the energy positions of spectral peaks (cf. Figure 4) is the half of the energy step size of the HR-XANES spectra, i.e. ± 0.05 eV. The U M₄ and M₅ edge VB-RIXS spectra were measured by using 3 Ge(311) or 3 Si(220) analyzer crystals, respectively. The incident excitation energy was set to the maximum of the first most intensive absorption feature of the U M₄/M₅ edge HR-XANES spectra. The analyzer crystal at 90° scattering geometry was Si(220) (for U M₄ VB-RIXS) or Ge(220) (for U M₅ VB-RIXS). It was used to measure U M₄ or M₅ HR-XANES spectra and M_β or M_α normal emission lines of a UO₂ reference and the compounds. The maximum intensity of this normal emission lines was used to normalize the VB-RIXS spectra so that their intensities can be compared. The experimental energy resolution measured as the full width at half maximum of the elastic scattering peak was 2,66 eV (M₅ VB-RIXS) and 1 eV (M₄ VB-RIXS). The VB-RIXS spectra were measured with 0.5 (M₄)/0.6 (M₅) edge step size.

Eight solid-state pellets ($d = 5$ mm, thickness = 1–2 mm) of all complexes (**1**–**8**) were prepared in an Ar glove box. Dried microcrystalline sample was finely ground with boron nitride (BN) in a mortar before pressing it into a pellet. The composition of each pellet was calculated to contain approximately 0.005 mmol of uranium with a final weight of 40 mg. All pellets were placed in a Plexiglas holder and covered with a Kapton film with 13 μm thickness. The Plexiglas holders were shipped in Schlenck tubes under Ar in heat sealed mylar bags. The holders were placed in an Ar glove box in an inert gas cell described in^[5] and transported to the beamline. A constant He flow was maintained through the inert gas cell during the measurements.

FDMNES computations. FDMNES is a DFT based *ab-initio* code, which calculates the electronic structure using the multiple scattering theory under the muffin-tin approximation on the potential shape. In the present study better results are obtained using the finite difference method allowing a free-shape potential. To obtain the absorption cross section, FDMNES first solves the electronic structure in the cluster probed by the photoelectron around the absorbing atom, giving thus the projected Density Of States (DOS) in the atoms. The calculations of the DOS and U M₄ and M₅ edge HR-XANES and X-ray emission spectra (XES) spectra are self-consistent, relativistic and include spin–orbit coupling. We found very good agreement between the ground state calculations and the spectra of complexes **1**, **2** and **3** as previously shown for plutonyl(VI) and neptunyl(V) and (VI), i.e. no core-hole is considered.^[4, 6] The experimental HR-XANES spectra closely follow the U f and p unoccupied DOS as expected from the selection rules. Peak C (σ^*) is at lower energy position in the experimental compared to computed spectra for the U(V) compounds **2** and **3** and the deviation appears stronger for the U M₅ edge. This can be explained with differences in screening of the 3d_{3/2}/4f_{5/2} (M₄ edge) and 3d_{5/2}/4f_{7/2} (M₅ edge) core-holes (cf. Figure 3 b). Peak B is not resolved in the U M₅ edge HR-XANES spectra. No experimental broadening is considered thus the computed spectra are better resolved than the experimental spectra. An example of the applied input file is given in SI. The O and N p – DOS and U d – DOS are shown in Figures S31 and S32. The XES spectra are obtained by setting the Fermi energy below the occupied valence band. Note that the selection rules for the U M₄ and M₅ edge electronic transitions summarized in Figure 2 b are considered also for the XES spectra. The coordinates of the atoms necessary for the calculations were previously published for complexes **1** and **2** complex (**1** –

CCDC 851298, **2** - CCDC 851300) and it is reported here for the first time for complex **3** (CCDC [2035745](#)). The DOS and HR-XANES/XES spectra were calculated for each U site in the unite cell (cf. SI Figure S29, S30). The spectra were then averaged to obtain the final spectra in Figure 3.

DFT and CASSCF computations. Geometry optimizations of all complexes have been performed using the B3PW91^[7] hybrid functional without any symmetry restrictions. The uranium, iron and potassium atoms were treated with its Stuttgart-Köln relativistic effective small core potential (RECP, 60MWB)^[8] meanwhile for H, C, N and O atoms with the 6-31G(d,p) basis sets.^[9] To further investigate the nature of the bond, Wiberg bond indices have been calculated using the natural bond orbital (NBO) scheme using NBO3.1, NBO 5 and NBO6.^[10] In order to analyze the electronic states of various uranium complexes we followed the same procedure as in our previous studies.^[11] In the first step, we have determined the optimal sets of molecular orbitals (MOs) for each complex through Restricted Open Shell (ROHF) calculations for different spin values (S=0, 1 and 2). In a second stage, using these MOs we have carried out a systematic Complete Active Space Self Consistent Field (CASSCF) study by checking the T1 value to determine the validity of our chosen MOs (in all cases it was below 0.005). The size of the active space was also checked by first distributing eight electrons in 9 orbitals (CAS(8,9)) then 7 electrons in seven orbitals (CAS(7,5)). It was found that the active space (CAS) could be safely reduced to distributing either four or five electrons in four or five active orbitals (CAS(5,5) or CAS(4,4)) with a similar description of the states. Note that for all complexes considered in this work, CASSCF computations have been carried out to elucidate the nature of the first and the second roots for each spin value aforementioned. All electronic structure calculations were carried out with Gaussian09 software.

References

- [1] V. Mougel, J. Pecaut, M. Mazzanti, *Chem. Commun.* **2012**, *48*, 868-870.
- [2] L. Chatelain, J. Pecaut, F. Tuna, M. Mazzanti, *Chemistry* **2015**, *21*, 18038-18042.
- [3] R. Faizova, R. Scopelliti, A. S. Chauvin, M. Mazzanti, *J Am Chem Soc* **2018**, *140*, 13554-13557.
- [4] A. Zimina, K. Dardenne, M. A. Denecke, D. E. Doronkin, E. Huttel, H. Lichtenberg, S. Mangold, T. Pruessmann, J. Rothe, T. Spangenberg, R. Steininger, T. Vitova, H. Geckeis, J. D. Grunwaldt, *Rev Sci Instrum* **2017**, *88*, 113113.
- [5] V. Häußler, S. Amayri, A. Beck, T. Platte, T. A. Stern, T. Vitova, T. Reich, *Applied Geochemistry* **2018**, *98*, 426-434.
- [6] T. Vitova, I. Pidchenko, D. Schild, T. Prussmann, V. Montoya, D. Fellhauer, X. Gaona, E. Bohnert, J. Rothe, R. J. Baker, H. Geckeis, *Inorg. Chem.* **2020**, *59*, 8-22.
- [7] aA. D. Becke, *J Chem Phys* **1993**, *98*, 5648-5652; bJ. P. Perdew, Y. Wang, *Phys Rev B Condens Matter* **1992**, *45*, 13244-13249.
- [8] B. P. Pritchard, D. Altarawy, B. Didier, T. D. Gibson, T. L. Windus, *J Chem Inf Model* **2019**, *59*, 4814-4820.
- [9] aW. J. Hehre, R. Ditchfield, J. A. Pople, *J Chem Phys* **1972**, *56*, 2257-2261; bA. D. McLean, G. S. Chandler, *J Chem Phys* **1980**, *72*, 5639-5648.

- [10] A. E. Reed, L. A. Curtiss, F. Weinhold, *Chem Rev* **1988**, *88*, 899-926.
- [11] aC. H. Booth, D. Kazhdan, E. L. Werkema, M. D. Walter, W. W. Lukens, E. D. Bauer, Y. J. Hu, L. Maron, O. Eisenstein, M. Head-Gordon, R. A. Andersen, *J Am Chem Soc* **2010**, *132*, 17537-17549; bC. H. Booth, M. D. Walter, D. Kazhdan, Y. J. Hu, W. W. Lukens, E. D. Bauer, L. Maron, O. Eisenstein, R. A. Andersen, *J Am Chem Soc* **2009**, *131*, 6480-6491; cR. L. Halbach, G. Nocton, J. I. Amaro-Estrada, L. Maron, C. H. Booth, R. A. Andersen, *Inorg Chem* **2019**, *58*, 12083-12098; dR. L. Halbach, G. Nocton, C. H. Booth, L. Maron, R. A. Andersen, *Inorg Chem* **2018**, *57*, 7290-7298.
- [12] R. Faizova, R. Scopelliti, A. S. Chauvin, M. Mazzanti, *Journal of the American Chemical Society* **2018**, *140*, 13554-13557.

1. General Considerations.

All manipulations were carried out under an inert argon atmosphere using an MBraun glovebox equipped with a purifier unit. The oxygen level was always kept at less than 0.1 ppm. The solvents were purchased from Aldrich or Cortecnet (deuterated solvents) in their anhydrous form and freeze-degassed. Depleted uranium was purchased from IBILABS, USA.

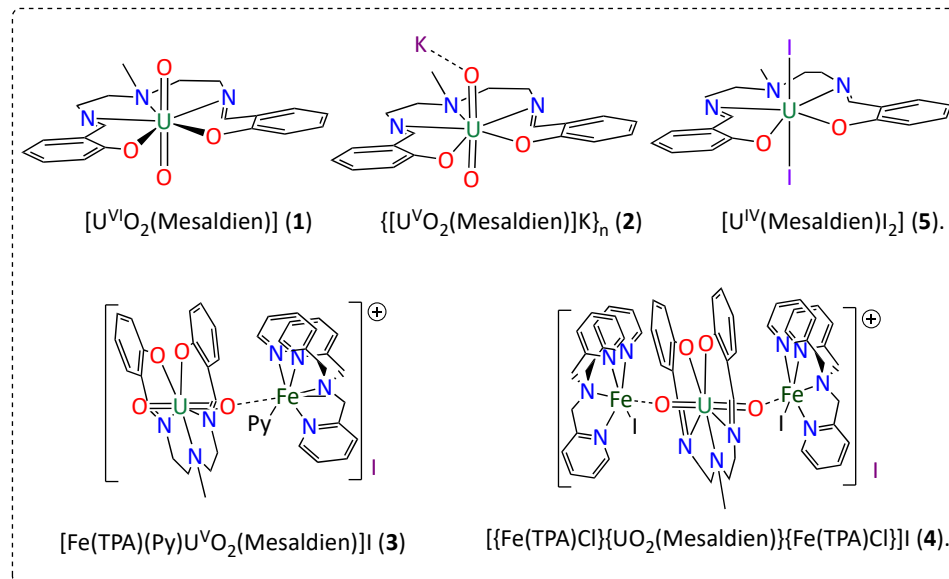
$[(\text{UO}_2\text{Py}_5)(\text{KI}_2\text{Py}_2)]_n$ ¹, $[\text{UI}_4(\text{dioxane})_{1.8}]^2$, K₂Mesaldien³, TPA⁴, H₂dpaea(HCl)₃⁵ were prepared according to the published procedures. UO₂(NO₃)₂(H₂O)₆ was purchased from Sigma-Aldrich. 2.2.2.cryptand (4,7,13,16,21,24-hexaoxa-1,10-diazabicyclo[8.8.8]hexacosane) was purchased from Aldrich and sublimated prior to use. FeI₂ was purchased from Aldrich and used without further purification.

Elemental analyses were performed under argon with a Thermo Scientific Flash 2000 Organic Elemental Analyzer by the EPFL elemental analyses service. ¹H NMR experiments were carried out using NMR tubes adapted with J. Young valves. ¹H NMR spectra were recorded on Bruker 400 MHz spectrometer. NMR chemical shifts are reported in ppm with solvent as internal reference.

Caution: Depleted uranium (primary isotope ^{238}U) is a weak α -emitter (4.197 MeV) with a half-life of 4.47×10^9 years. Manipulations and reactions should be carried out in monitored fume hoods or in an inert atmosphere glovebox in a radiation laboratory equipped with α - and β -counting equipment.

2. Experimental Procedures

Synthesis of coordination complexes of Mesaldien²⁻ ligand.



Complexes **1** and **2** were prepared as previously described.³ Complex **4** was prepared according to a previously published procedure for preparation of $\{[\text{Fe}(\text{TPA})\text{Cl}]\{\text{UO}_2(\text{Mesaldien})\}\{\text{Fe}(\text{TPA})\text{Cl}\}\}\text{I}$.⁶ The U M₄ edge high energy resolution X-ray absorption near edge structure (HR-XANES) spectrum was measured for $\{[\text{Fe}(\text{TPA})\text{I}]\{\text{UO}_2(\text{Mesaldien})\}\{\text{Fe}(\text{TPA})\text{I}\}\}\text{I}$ (**4** (X=I)) while no X-ray crystal structure of

4 (X=I) was obtained. Metric parameters from **4** (X=Cl) were used for structural comparison. Synthesis for two novel compounds **3** and **5** is presented below.

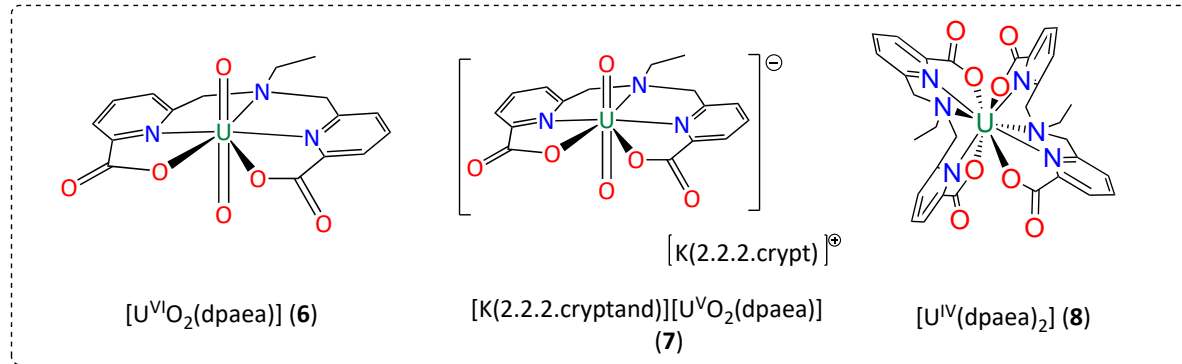
Synthesis of [Fe(TPA)(Py)U^VO₂(Mesaldien)]I (3).

An orange suspension of [Fe(TPA)I₂] prepared *in situ* from the reaction of FeI₂ (11.1 mg, 0.036 mmol, 1 equiv.) with TPA (10.5 mg, 0.036 mmol, 1 equiv.) in 1 mL of pyridine is added to a stirred dark blue solution of {[U^VO₂(Mesaldien)]K}_n prepared *in situ* from the reaction of [(UO₂Py₅)(KI₂Py₂)]_n (40.0 mg, 0.036 mmol, 1 equiv.) with K₂Mesaldien (14.4 mg, 0.036 mmol, 1 equiv.) in 2 mL of pyridine. Immediately the resulting solution changes colour to dark red. The reaction mixture was stirred overnight. Resulting solution was filtered and X-ray quality crystals of [Fe(TPA)(Py)UO₂(Mesaldien)]I (26.5 mg, 0.022 mmol, 60%) were obtained by slow diffusion of hexane. Elemental analysis calcd (%) for [Fe(TPA)(Py)UO₂(Mesaldien)]I.(KI)₁ (C₃₇H₃₉I₂N₇O₄FeK₁U MW=1232.545) 36.06; H, 3.19; N, 7.95. Found: C, 35.84; H, 2.78; N, 7.63

Synthesis of [UI₂(Mesaldien)] (5).

A solution of 43.6 mg of [UI₄(dioxane)_{1.8}] (0.05 mmol, 1 equiv.) in pyridine (1.5 mL) was added to a suspension of 19.4 mg of K₂Mesaldien (0.05 mmol, 1 equiv.) in 1.5 mL of pyridine yielding after 15 minutes a dark red solution, that was filtered and set for crystallization. 31 mg (0.036, 72%) of dark red crystals suitable for X-Ray of [UI₂(Mesaldien)] were collected after slow diffusion of 1,4-dioxane or DIPE. ¹H NMR (200 MHz, C₅D₅N, 298 K): δ = 96.34 (s, 2H), 43.26 (s, 2H), 30.80 (s, 2H), 24.36 (d, 4H), 17.96 (s, 2H), 15.46 (s, 2H), -2.08 (s, 3H), -26.54 (s, 2H), -37.76 (s, 2H). Elemental analysis (%) calcd for [UI₂(Mesaldien)].0.17 KI C₁₉H₂₁I₂N₃O₂U(KI)_{0.17}: C, 27.06; H, 2.51; N, 4.98. Found: C, 26.65; H, 2.92; N, 5.10

Synthesis of coordination complexes of dpaea²⁻ ligand.



Complexes **6**, **7** and **8** were prepared according to a previously published procedure.⁷

3. NMR spectra

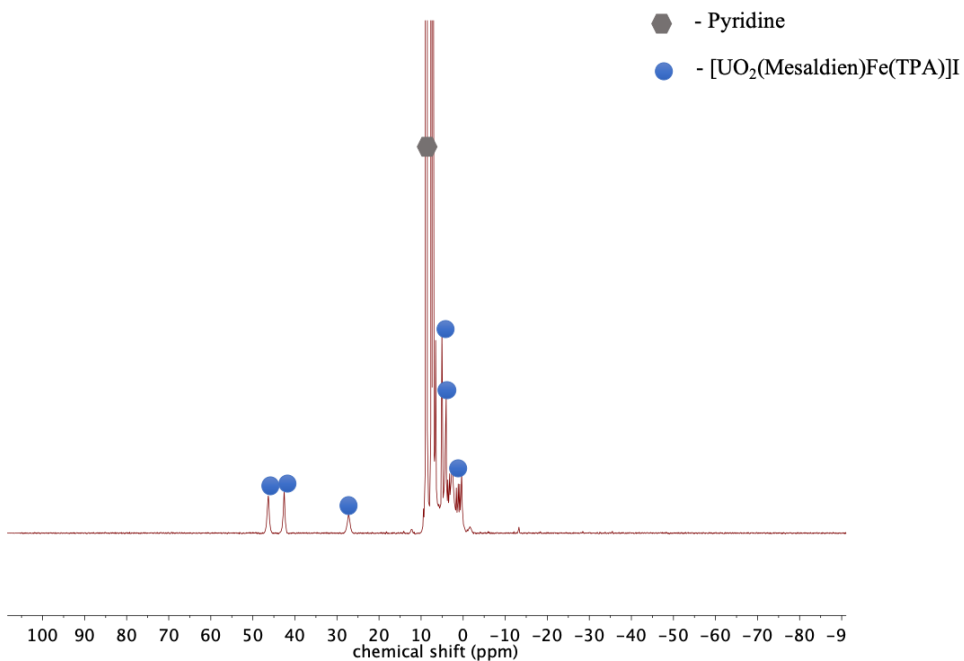


Figure S1. ¹H NMR (400MHz, C₅D₅N, 298K) of complex [Fe(TPA)(Py)U^VO₂(Mesaldien)]I (**3**).

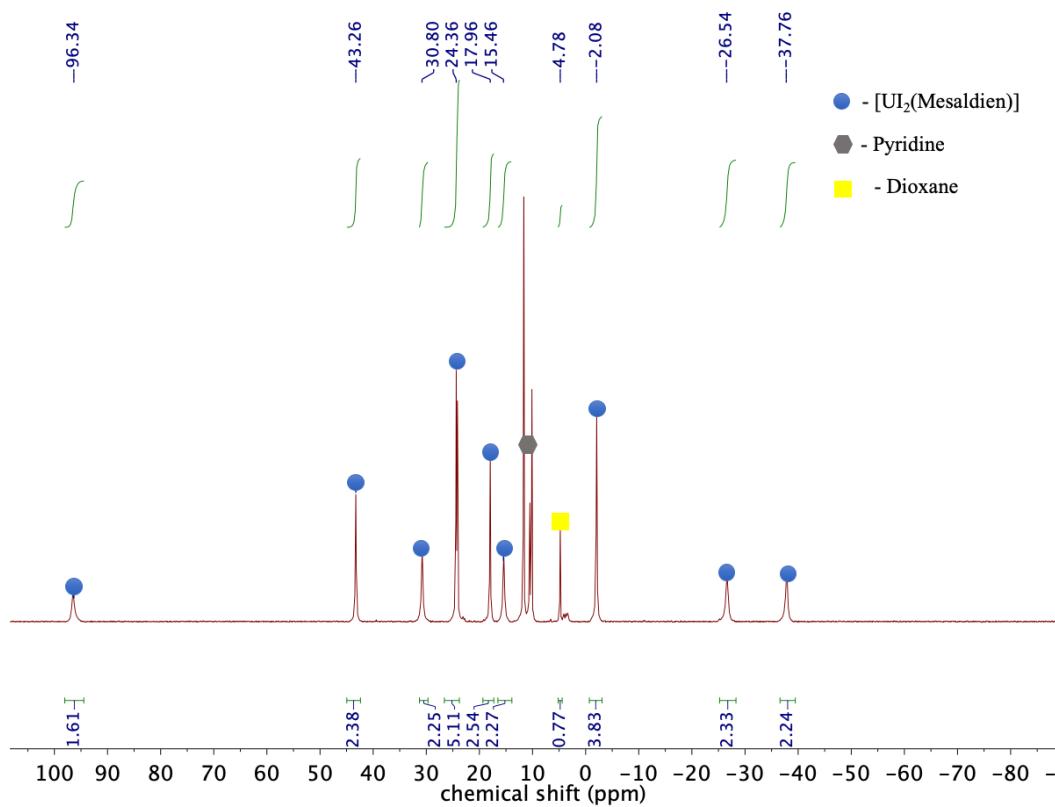
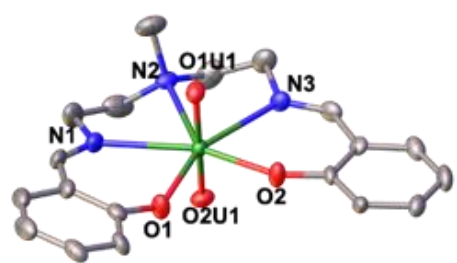


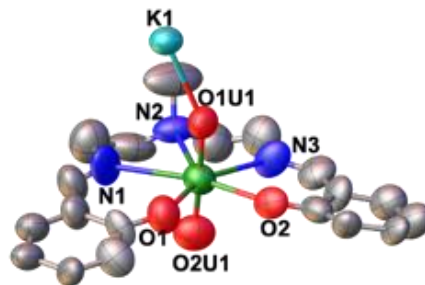
Figure S2. ^1H NMR (400MHz, $\text{C}_5\text{D}_5\text{N}$, 298K) of complex $[\text{UI}_2(\text{Mesaldien})]$ (5).

4. Crystallographic data

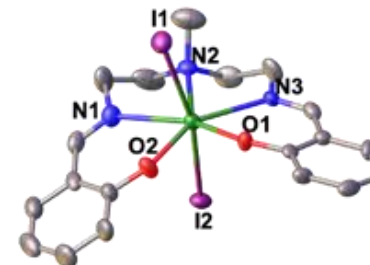
Bragg-intensities of **3** and **5** were collected at 140 K using CuK α radiation. A Rigaku SuperNova dual system diffractometer with an Atlas CCD detector was used for compound **3**, and one equipped with an Atlas S2 CCD detector for compound **5**. The datasets were reduced and corrected for absorption, with the help of a set of faces enclosing the crystals as snugly as possible, with *CrysAlis^{Pro}*.⁸ The solutions and refinements of the structures were performed by the latest available version of *ShelXT*⁹ and *ShelXL*.¹⁰ All non-hydrogen atoms were refined anisotropically using full-matrix least-squares based on $|F|^2$. The hydrogen atoms were placed at calculated positions by means of the “riding” model where each H-atom was assigned a fixed isotropic displacement parameter with a value equal to 1.2 U_{eq} of its parent C-atom (1.5 U_{eq} for the methyl groups). Crystallographic and refinement data are summarized in Table S1. The CCDC numbers 2035745 and 2035746 for compounds **3** and **5** contain the supplementary crystallographic data for this paper. These data can be obtained free of charge via www.ccdc.cam.ac.uk/data_request/cif



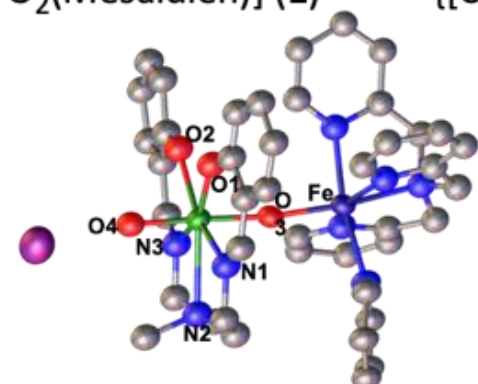
$[\text{U}^{\text{VI}}\text{O}_2(\text{Mesaldien})] \text{ (1)}$



$\{[\text{U}^{\text{V}}\text{O}_2(\text{Mesaldien})]\text{K}\}_n \text{ (2)}$

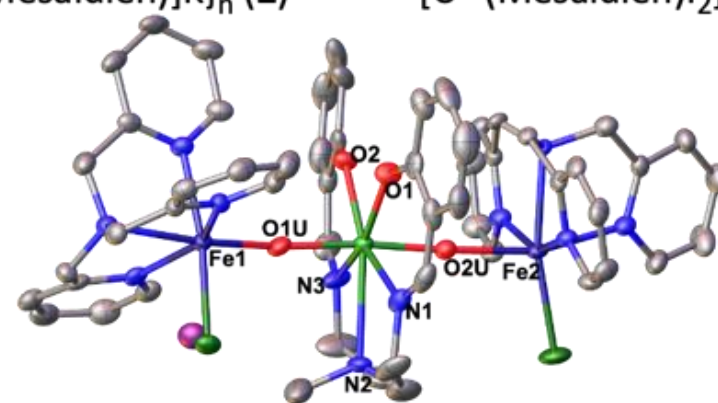


$[\text{U}^{\text{IV}}(\text{Mesaldien})\text{I}_2] \text{ (5)}$.



$[\text{Fe}(\text{TPA})(\text{Py})\text{U}^{\text{V}}\text{O}_2(\text{Mesaldien})]\text{I} \text{ (3)}$

f.



$\{[\text{Fe}(\text{TPA})\text{Cl}]\{\text{UO}_2(\text{Mesaldien})\}\{\text{Fe}(\text{TPA})\text{Cl}\}\}\text{I} \text{ (4)}$

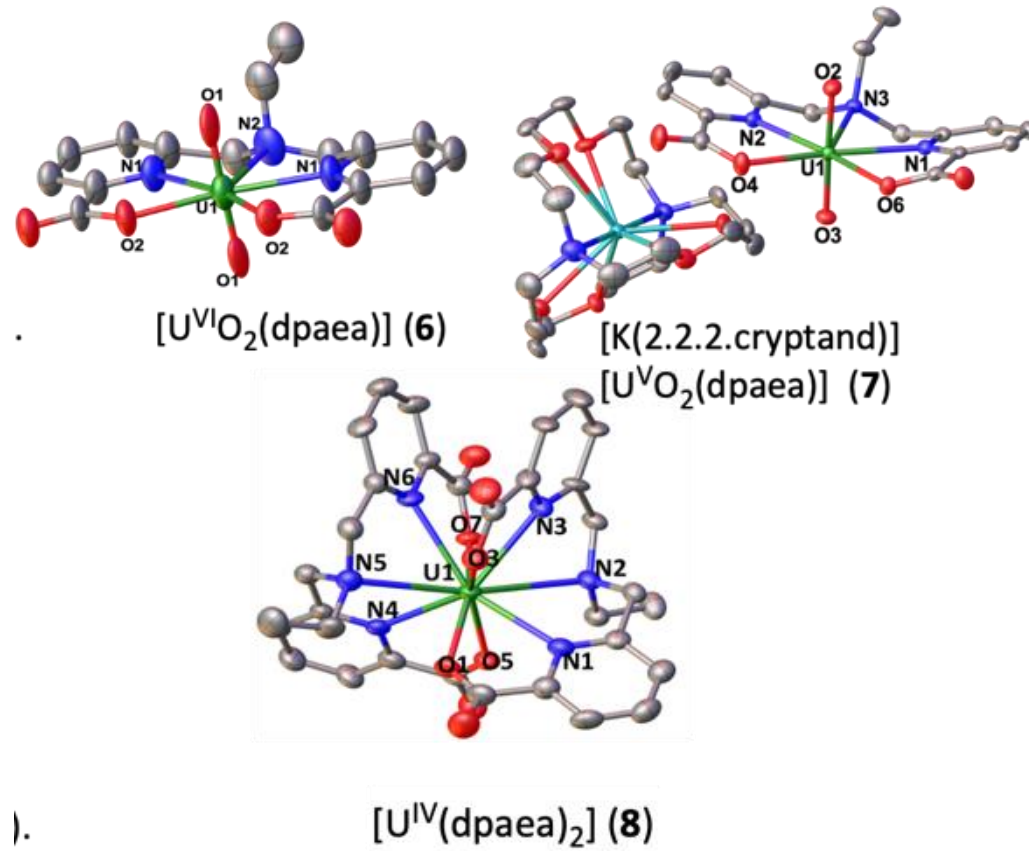


Figure S3. Ellipsoid plot at 50% probability of X-ray molecular structures of complexes 1-8.

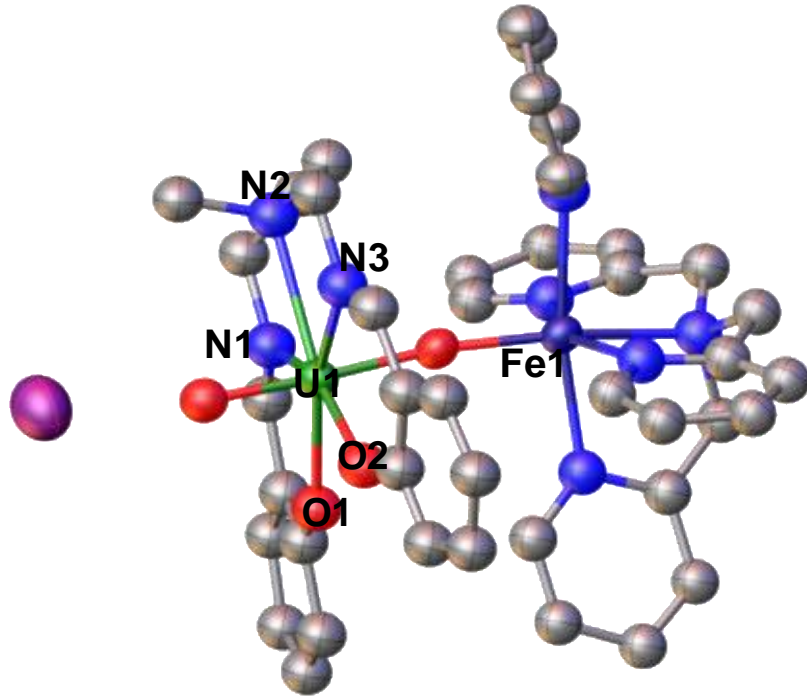


Figure S4. Ellipsoid plot at 50 % probability of complex 3 (the solvent molecules of pyridine and H were omitted for clarity, C are represented in grey, O in red, N in blue, Fe in dark blue, I in purple and U in green).

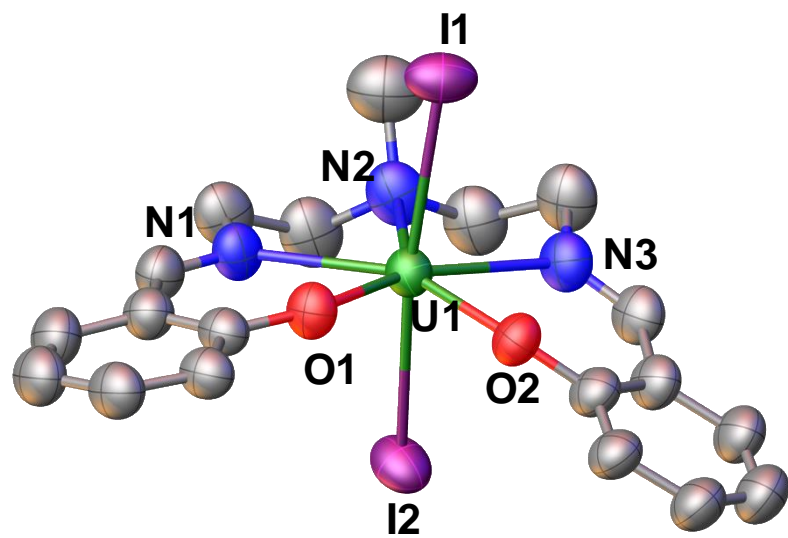


Figure S5. Ellipsoid plot at 50 % probability of complex 5 (the solvent molecules of pyridine and H were omitted for clarity, C are represented in grey, O in red, N in blue, I in purple and U in green).

Table S1. Crystallographic data of 3 and 5.

	3	5
Formula	C ₂₃₃ H ₂₄₁ Fe ₄ I ₁₀ N ₄₅ O ₁₆ U ₄	C ₁₉ H ₂₁ I ₂ N ₃ O ₂ U
Crystal size (mm ³)	0.324 × 0.249 × 0.184	0.37×0.24×0.12
cryst syst	monoclinic	Orthorhombic
space group	P2 ₁ /n	Pbca
volume (Å ³)	24459.4(7)	13739.73(15)
a (Å)	21.8709(4)	17.56258(11)
b (Å)	18.1771(3)	17.06374(11)
c (Å)	61.5667(10)	45.8475(3)
α (deg)	90	90
β (deg)	92.0956(16)	90
γ (deg)	90	90
Z	4	3
formula weight (g/mol)	6372.21	815.22
density (g cm ⁻³)	1.730	2.365
absorption coefficient (mm ⁻¹)	19.637	41.267
F(000)	12336.0	732
temp (K)	140.00(10)	139.99(10)
total no. reflections	160741	154881
unique reflections [R(int)]	43066 [R _{int} = 0.1034]	14336 [0.1229]
Final R indices	R ₁ = 0.1655,	R ₁ = 0.0650,

[I > 2σ(I)]	wR ₂ = 0.3615	wR ₂ = 0.1775
Largest diff. peak and hole (e.A ⁻³)	5.93 and -4.28	5.859 and -2.227
GOOF	1.158	1.097
CCDC number	2035745	20357456

5. Molecular structures description.

[U^{VI}O₂(Mesaldien)] (1).³ The structure of **1** consists of a typical U(VI)-yl Schiff base complex, with two crystallographically inequivalent U(VI)-yl cations coordinated by the three N and two O atoms of the ligand in their equatorial plane, and the U atoms at the center of a slightly distorted pentagonal bipyramid. The O=U=O angle is 173.31(14)°. In this complex, the mean bond distances (U=O (1.77(1) Å), U-O(phen) (2.22(1) Å), U-N(imine) (2.58(2) Å) and U-N(amine) (2.613(4) Å)) lie in the range of the values observed for uranyl(VI) complexes.

{[U^{VI}O₂(Mesaldien)]K}_n (2).³ The structure of polymer **2** consists of [UO₂(Mesaldien)] anions connected through K cations binding two uranyl oxygens from adjacent complexes to form a ladder-like chain. The two crystallographically independent U atoms in **2** are seven-coordinated, with a slightly distorted pentagonal bipyramidal geometry, by two trans oxo groups, three N and two O from the Schiff base ligand. The O=U=O angle at 177.4(8)° is more linear compared to **1**. In this complex, the mean U=O bond distances lie in the range of the values observed for U(V)-yl complexes, with the UO₂⁺.....K⁺ interaction resulting in a slight lengthening of the U=O bonds (average U=O = 1.84(2) Å) with respect to unbound O (average U=O=1.787(1) Å). The mean values of U-O(phen) (2.35(4) Å), U-N(imine) (2.62(3) Å) and U-N(amine) (2.67(3) Å) also lie in the range of values observed for U(V)-yl complexes.

[Fe(TPA)(Py)U^VO₂(Mesaldien)]I (3). The structure of complex **3** as determined by X-Ray crystallography consists of [{Fe(TPA)(Py)}{UO₂(Mesaldien)}] cations and Iodide anions. The Fe(II) from the cationic {Fe(TPA)(Py)} unit binds an oxo group from the {UO₂(Mesaldien)} moiety in a linear cation–cation interaction. In this compound the U atom is hepta-coordinate with a slightly distorted pentagonal bipyramidal geometry by two uranyl oxygen atoms and five donor atoms of the Mesaldien²⁻ ligand in the equatorial plane. The Fe center is hexa-coordinated, with a slightly distorted octahedral geometry defined by four N atoms of the TPA ligand, one N atom of the pyridine molecule and one O atom of the uranyl group. On coordination of Fe²⁺ the U-O(yl) bond is significantly elongated with respect to the second unbound U-O(yl) bond (1.95(2) Å vs. 1.84(2) Å). The O=U=O angle remains unchanged compared to complex **2**. The U-O and U-N distances of the U^V(Mesaldien) moiety are also similar to those found in **2** (U-O(phen) (2.28(2) Å), U-N(imine) (2.59(1) Å) and U-N(amine) (2.62(3) Å)).

[{Fe(TPA)X}{UO₂(Mesaldien)}{Fe(TPA)X}]I (4). The previously reported structure³ of **4** (X=Cl) shows a trinuclear [{Fe(TPA)X}{UO₂(Mesaldien)}{Fe(TPA)X}]⁺ cation fragment with an outer-sphere iodide counterion. The arrangement of three metal ions in the Fe(II)-O=U(V)=O-Fe(II) CCI is almost linear (173.5401(1) $^{\circ}$) whith two {Fe(TPA)X}⁺ cations binding the two oxo groups of the {UO₂(Mesaldien)} moiety. In this complex the U in the {UO₂(Mesaldien)} moiety retains the coordination environment found in **2** and **3** with analogous U-Mesaldien bond distances. The Fe(II) cation is hexacoordinated by the four N atoms of the TPA ligand, one O atom of the uranyl(V) group, and a Cl⁻ anion. As for the complex **3**, the Fe²⁺ binding to the uranyl(V)-oxo groups results in an elongation of the U-O(yl) bonds compared to the unbound analogue (1.877(4) Å (**4**) vs. 1.84(2) (**3**) Å).

[U^{IV}I₂(Mesaldien)] (5). The structure of **5** consists of a seven-coordinated U atom with a distorted pentagonal bipyramidal geometry. The axial arrangement of I-U-I deviates from planarity (176(3) $^{\circ}$) with an average U-I bond length of U-I being 3.04(2) Å. The equatorial

Mesaldien²⁻ ligand significantly deviates from planarity (RMSD/A= 0.09) with the mean values of U-O(phen) (2.134(16) Å), U-N(imine) (2.575(15) Å) and U-N(amine) (2.67(3) Å) being consistent with U(IV) oxidation state.

[U^{VI}O₂(dpaea)] (6).⁷ The molecular structure of **6** shows the presence of a U(VI) cation hepta-coordinated, with a slightly distorted pentagonal bipyramidal geometry, by the three nitrogen and two oxygen atoms of the dianionic pentadentate ligand dpaea²⁻ in the equatorial plane and by two oxo groups in axial position with values of U=O bond distances of 1.75(3) Å. The arrangement of the ligand is perfectly planar for the complex **6**. The O=U=O angle is 176.9(7)°. The mean values of the bonds in the equatorial plane are U-O(carbox) (2.310(13) Å), U-N(pyr) (2.46(2) Å) and U-N(amine) (2.64(2) Å).

[K(2.2.2.cryptand)][U^VO₂(dpaea)] (7).^{7 [12][12][12]} The structure of the [UO₂(dpaea)]⁻ anion shows the presence of a U(V) cation hepta-coordinated, with a pentagonal bipyramidal geometry, by two trans oxo groups and by five coplanar O₂N₃ donor atoms of the dpaea²⁻ ligand. The O=U=O angle remains unchanged compared to the U(VI) analogue **6** (176.5(6)°). The U=O bond distances in **7** (1.843(6) Å) are significantly longer compared to **6**, which is in agreement with the presence of a reduced U center. The mean values of the bonds in the equatorial plane (U-O(carbox) 2.456(4) Å, U-N(pyr) 2.574(1) Å and U-N(amine) 2.696(2) Å) are also longer than those found in **6** and are consistent with the presence of a U(V) complex.

[U^{IV}(dpaea)₂] (8).⁷ The structure of [U^{IV}(dpaea)₂] shows an uranium cation encapsulated by two pentadentate ligands resulting in a N₆O₄ coordination pocket arranged in a distorted bicapped square antiprism geometry. The average U-O, U-N(pyr) and U-N(amine) bond lengths are 2.309(5) Å, 2.309(5) Å and 2.969(6) Å respectively. Due to the flexibility of the dpaea²⁻ ligand a nearly orthogonal angle is formed in between two 2 picolinate arms of each ligand.

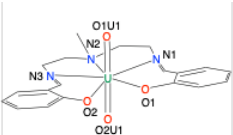
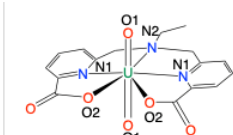
Molecule				
Formula	[UO ₂ (Mesaldien)] 1	[UO ₂ (dpaea)] 6		
Name	Uranyl(VI) Mesaldien	Uranyl(VI) dpaea		
U-O(yl)/U-O(yl)M+	bond (U1-O1U1) Å	1.784(3)	bond (U1-O1) Å	1.75(3)
U-O(yl)	bond (U1-O2U1) Å	1.779(3)		
U-O(phen/carbox)	bond (U1-O1) Å	2.218(3)	bond (U1-O2) Å	2.310(13)
U-O(phen/carbox)	bond (U1-O2) Å	2.218(3)		
U-N(imine/pyr))	bond (U1-N1) Å	2.604(4)	bond (U1-N1) Å	2.46(2)
U-N(amine)	bond (U1-N2) Å	2.609(4)	bond (U1-N2) Å	2.64(2)
U-N(imine/pyr))	bond (U1-N3) Å	2.578(4)		

Table S2. Comparison of bond lengths in complexes **1** and **6**.

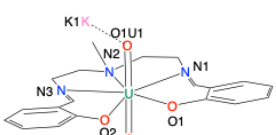
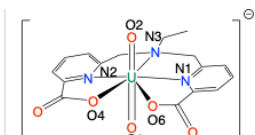
Molecule				
Formula	[KUO ₂ (Mesaldien)] 2	[K(2.2.2.crypt)][UO ₂ (dpaea)] 7		
Name	Uranyl(V) Mesaldien	Uranyl(V) dpaea		
U-O(yl)/U-O(yl)M+	bond (U1-O1U1) Å	1.86(2)	bond (U1-O2) Å	1.847
U-O(yl)	bond (U1-O2U1) Å	1.79(2)	bond (U1-O3) Å	1.838
U-O(phen/carbox)	bond (U1-O1) Å	2.398(15)	bond (U1-O4) Å	2.459
U-O(phen/carbox)	bond (U1-O2) Å	2.318(19)	bond (U1-O6) Å	2.453
U-N(imine/pyr))	bond (U1-N1) Å	2.63(2)	bond (U1-N1) Å	2.573
U-N(amine)	bond (U1-N2) Å	2.65(3)	bond (U1-N2) Å	2.575
U-N(imine/pyr))	bond (U1-N3) Å	2.57(2)	bond (U1-N3) Å	2.696
O(yl)-M+	bond (O1U1-K1)	2.76		

Table S3. Comparison of bond lengths in complexes **2** and **7**.

[KUO ₂ (Mesaldien)] 2		[Fe(tpa)UO ₂ (Mesaldien)]I 3	[Fe ₂ (tpa) ₂ UO ₂ (Mesaldien)]I ₂ ⁺ 4	
Uranyl(V) Mesaldien		1Fe(II)- Uranyl(V) Mesaldien	2Fe(II)- Uranyl(V) Mesaldien	
U-O(yl)/U-O(yl)M+	bond (U1-O1U1) A	1.86(2)	bond (U1-O1U) A	1.917(4)
U-O(yl)	bond (U1-O2U1) A	1.79(2)	bond (U1-O2U) A	1.877(4)
U-O(phen/carbox)	bond (U1-O1) A	2.398(15)	bond (U1-O1) A	2.265(4)
U-O(phen/carbox)	bond (U1-O2) A	2.318(19)	bond (U1-O2) A	2.257(4)
U-N(imine/pyr)	bond (U1-N1) A	2.63(2)	bond (U1-N1) A	2.591(5)
U-N(amine)	bond (U1-N2) A	2.65(3)	bond (U1-N2) A	2.638(4)
U-N(imine/pyr)	bond (U1-N3) A	2.57(2)	bond (U1-N3) A	2.596(5)
O(yl)-M+	bond (O1U1-K1)	2.76	bond (O3-Fe1)	1.998(4)
O(yl)-M+			bond (O2U-Fe2)	2.132(4)

Table S4. Comparison of bond lengths in complexes **2**, **3** and **4**.

		[UO ₂ (Mesaldien)]	[U ^{IV} (Mesaldien)]I ₂		
		Uranyl(VI) Mesaldien	U(IV)Mesaldien		
Crystallographic names	To be used for description	Crystallographic names	To be used for description		
bond (U1-O1U1) A	U-O(yl)	1.784(3)	bond (U1-I1) A	U-I	3.04(2)
bond (U1-O2U1) A	U-O(yl)	1.779(3)	bond (U1-I2) A	U-I	3.04(2)
bond (U1-O1) A	U-O(phen)	2.218(3)	bond (U1-O1) A	U-O(phen)	2.134(16)
bond (U1-O2) A	U-O(phen)	2.218(3)	bond (U1-O2) A	U-O(phen)	2.134(16)
bond (U1-N1) A	U-N(imine)	2.604(4)	bond (U1-N1) A	U-N(imine)	2.575(15)
bond (U1-N2) A	U-N(amine)	2.609(4)	bond (U1-N2) A	U-N(amine)	2.67(3)
bond (U1-N3) A	U-N(imine))	2.578(4)	bond (U1-N3) A	U-N(imine))	2.575(15)

Table S5. Comparison of bond lengths in complexes **1** and **5**.

6. Computational details

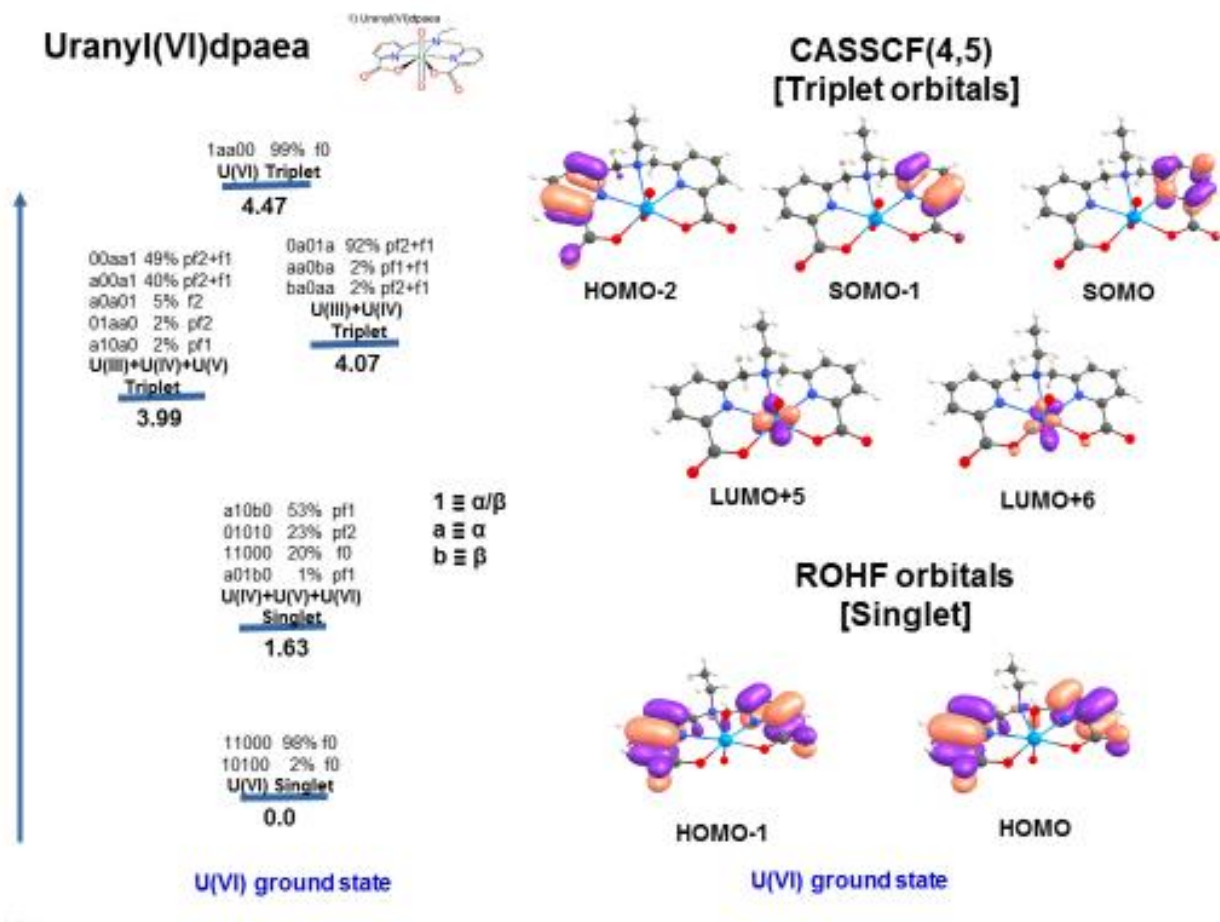


figure S6. CASSCF computed energy spectrum and depiction of the chooses active orbitals for complex 6

Singlet

Natural charges obtained at UB3PW91/6 -31G(d,p) level

Atom	Charge	Atom	Charge
C1	0.23213	O22	-0.52286
N2	-0.44339	O23	-0.52167
C3	0.16288	O24	-0.59795
C4	-0.23839	C25	-0.29456
C5	-0.18490	C26	-0.73613
C6	-0.26664	H27	0.28797
U7	1.52032	H28	0.26400
O8	-0.63439	H29	0.26031
C9	0.81854	H30	0.24360
O10	-0.59790	H31	0.28111
C11	0.81847	H32	0.28096
O12	-0.63445	H33	0.24350
C13	-0.30437	H34	0.26029
N14	-0.48847	H35	0.26398
C15	-0.30407	H36	0.28794
C16	0.23224	H37	0.26815
N17	-0.44316	H38	0.26799
C18	0.16272	H39	0.26858
C19	-0.23839	H40	0.23877
C20	-0.18497	H41	0.23887
C21	-0.26664		

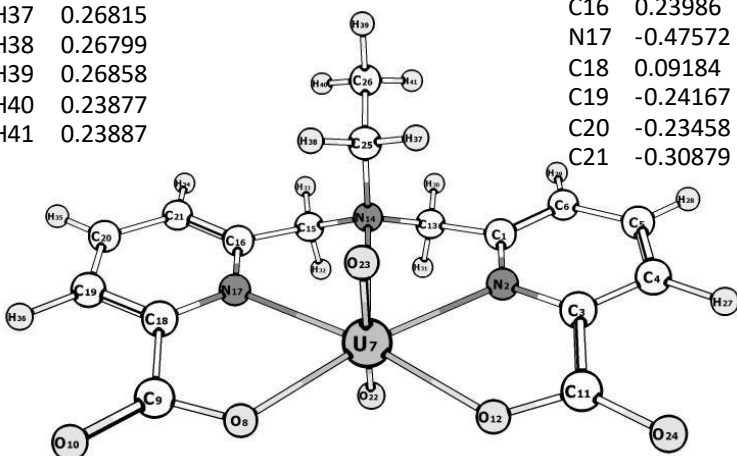


Figure S7. NPA Charges for complex 6

Quintet

Natural charges obtained at UB3PW91/6 -31G(d,p) level

Atom	Charge	Atom	Charge
C1	0.23956	O22	-0.55993
N2	-0.47600	O23	-0.56350
C3	0.09176	O24	-0.22959
C4	-0.24151	C25	-0.29466
C5	-0.23481	C26	-0.73449
C6	-0.30867	H27	0.26257
U7	1.46531	H28	0.25826
O8	-0.59758	H29	0.25334
C9	0.71644	H30	0.24056
O10	-0.22956	H31	0.27739
C11	0.71672	H32	0.27728
O12	-0.59753	H33	0.24048
C13	-0.30170	H34	0.25332
N14	-0.48900	H35	0.25826
C15	-0.30141	H36	0.26256
C16	0.23986	H37	0.26787
N17	-0.47572	H38	0.26766
C18	0.09184	H39	0.26358
C19	-0.24167	H40	0.23794
C20	-0.23458	H41	0.23813
C21	-0.30879		

Molecular Orbital energy levels obtained at UB3PW91/6-31G(d,p) level (Energy in a.u.).

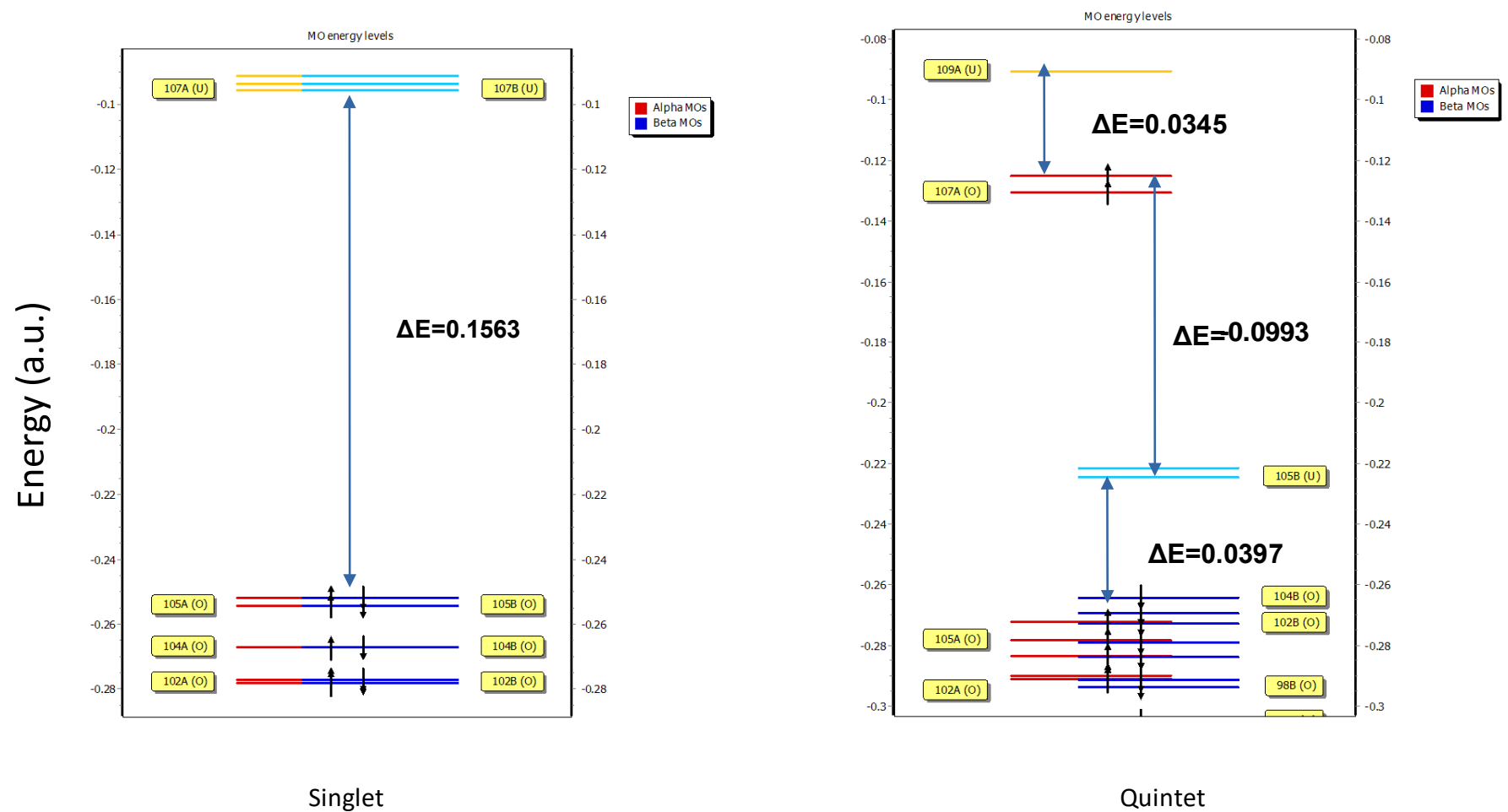
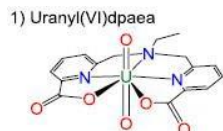


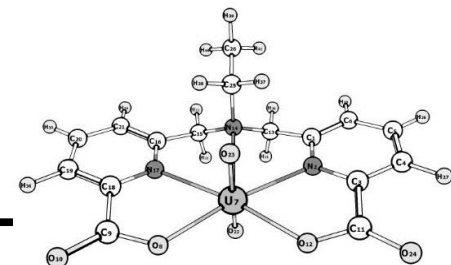
Figure S8. DFT computed energy spectrum for complex 6

Uranyl(VI)dpaea



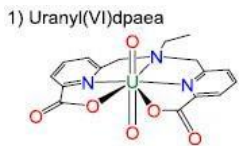
NBO Analysis obtained at UB3PW91/6 -31G(d,p) level (**alpha and beta spin orbitals**)

Singlet



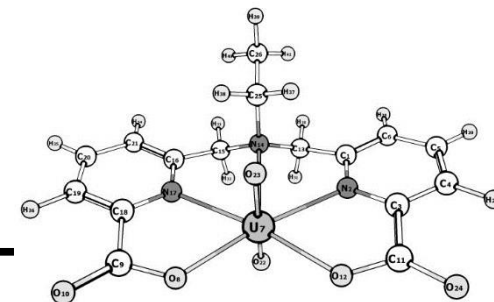
Donor Lewis -type NBO	Occupancy	Composition
(alpha spin) BD (1) U7 -O22	0.99350	(21.42%) 0.4628*U7 s(0.03%)p46.79(1.30%)d99.99(48.85%)f99.99(49.72%)g 3.74(0.10%) (78.58%) 0.8865*O22 s(0.09%)p99.99(99.67%)d 2.53(0.23%)
BD (2) U7 -O22	0.99316	(21.19%) 0.4604*U7 s(0.00%)p 1.00(0.45%)d99.99(48.39%)f99.99(51.06%)g 0.22(0.10%) (78.81%) 0.8877*O22 s(0.00%)p 1.00(99.77%)d 0.00(0.23%)
BD (3) U7 -O22	0.95943	(23.14%) 0.4811*U7 s(0.15%)p 2.44(0.37%)d99.99(49.61%)f99.99(49.58%)g 1.86(0.28%) (76.86%) 0.8767*O22 s(26.40%)p 2.78(73.31%)d 0.01(0.28%)
BD (1) U7 -O23	0.99945	(21.40%) 0.4626*U7 s(0.00%)p 1.00(0.99%)d48.62(48.26%)f51.01(50.64%)g 0.10(0.10%) (78.60%) 0.8866*O23 s(0.01%)p 1.00(99.76%)d 0.00(0.24%)
BD (2) U7 -O23	0.99388	(21.22%) 0.4607*U7 s(0.00%)p 1.00(0.54%)d89.17(48.09%)f95.05(51.27%)g 0.18(0.10%) (78.78%) 0.8876*O23 s(0.00%)p 1.00(99.77%)d 0.00(0.23%)
BD (3) U7 -O23	0.95748	(23.20%) 0.4817*U7 s(0.16%)p 2.63(0.43%)d99.99(49.57%)f99.99(49.54%)g 1.75(0.29%) (76.80%) 0.8763*O23 s(26.55%)p 2.76(73.17%)d 0.01(0.28%)
(beta spin) BD (1) U7 -O22	0.99350	(21.42%) 0.4628*U7 s(0.03%)p46.79(1.30%)d99.99(48.85%)f99.99(49.72%)g 3.74(0.10%) (78.58%) 0.8865*O22 s(0.09%)p99.99(99.67%)d 2.53(0.23%)
BD (2) U7 -O22	0.99316	(21.19%) 0.4604*U7 s(0.00%)p 1.00(0.45%)d99.99(48.39%)f99.99(51.06%)g 0.22(0.10%) (78.81%) 0.8877*O22 s(0.00%)p 1.00(99.77%)d 0.00(0.23%)
BD (3) U7 -O22	0.95943	(23.14%) 0.4811*U7 s(0.15%)p 2.44(0.37%)d99.99(49.61%)f99.99(49.58%)g 1.86(0.28%) (76.86%) 0.8767*O22 s(26.40%)p 2.78(73.31%)d 0.01(0.28%)
BD (1) U7 -O23	0.99454	(21.40%) 0.4626*U7 s(0.00%)p 1.00(0.99%)d48.62(48.26%)f51.01(50.64%)g 0.10(0.10%) (78.60%) 0.8866*O23 s(0.01%)p 1.00(99.76%)d 0.00(0.24%)
BD (2) U7 -O23	0.99388	(21.22%) 0.4607*U7 s(0.00%)p 1.00(0.54%)d89.17(48.09%)f95.05(51.27%)g 0.18(0.10%) (78.78%) 0.8876*O23 s(0.00%)p 1.00(99.77%)d 0.00(0.23%)
BD (3) U7 -O23	0.95748	(23.20%) 0.4817*U7 s(0.16%)p 2.63(0.43%)d99.99(49.57%)f99.99(49.54%)g 1.75(0.29%) (76.80%) 0.8763*O23 s(26.55%)p 2.76(73.17%)d 0.01(0.28%)

Uranyl(VI)dpaea

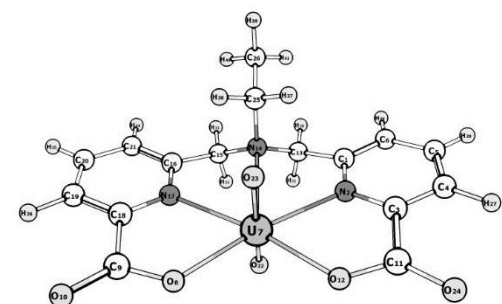
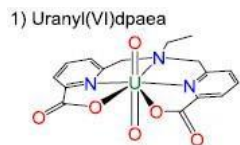


NBO analysis obtained at UB3PW91/6 -31G(d,p) level (**Alpha spin orbitals**).

Quintet



Donor Lewis -type NBO	Occupancy	Composition
BD (1) N2 -U7	0.96719	(89.47%)0.9459* N2 s(30.75%)p 2.25(69.23%)d 0.00(0.02%) (10.53%)0.3244* U7 s(16.04%)p 1.86(29.76%)d 1.94(31.17%)f 1.43(23.02%)g 0.00(0.01%)
BD (1) U7 -O8	0.98103	(10.15%)0.3186*U7 s(12.23%)p 1.95(23.86%)d 3.26(39.93%)f 1.96(23.95%)g 0.00(0.03%) (89.85%)0.9479*O8 s(46.46%)p 1.15(53.53%)d 0.00(0.01%)
BD (2) U7 -O8	0.91020	(7.39%)0.2719*U7 s(0.20%)p24.95(5.01%)d52.97(10.64%)f99.99(84.10%)g 0.27(0.05%) (92.61%)0.9623* O8 s(0.01%)p 1.00(99.91%)d 0.00(0.08%)
BD (1) U7 -O12	0.98100	(10.14%)0.3185*U7 s(12.23%)p 1.96(23.92%)d 3.26(39.92%)f 1.95(23.90%)g 0.00(0.03%) (89.86%)0.9479*O12 s(46.43%)p 1.15(53.56%)d 0.00(0.01%)
BD (2) U7 -O12	0.90997	(7.34%)0.2710*U7 s(0.21%)p24.62(5.05%)d52.32(10.74%)f99.99(83.95%)g 0.27(0.05%) (92.66%)0.9626*O12 s(0.01%)p 1.00(99.91%)d 0.00(0.08%)
BD (1) U7 -N14	0.95888	(7.79%)0.2790*U7 s(16.07%)p 1.30(20.97%)d 2.92(46.88%)f 1.00(16.08%)g 0.00(0.01%) (92.21%)0.9603*N14 s(19.37%)p 4.16(80.61%)d 0.00(0.02%)
BD (1) U7 -N17	0.96721	(10.52%)0.3244*U7 s(16.03%)p 1.86(29.75%)d 1.95(31.19%)f 1.44(23.02%)g 0.00(0.01%) (89.48%)0.9459*N17 s(30.72%)p 2.25(69.26%)d 0.00(0.02%)
BD (1) U7 -O22	0.98481	(19.46%) 0.4411*U7 s(0.02%)p99.99(4.93%)d99.99(42.18%)f99.99(52.73%)g 6.40(0.14%) (80.54%)0.8974*O22 s(0.06%)p99.99(99.72%)d 3.63(0.22%)
BD (2) U7 -O22	0.98658	(20.88%)0.4569*U7 s(0.55%)p 6.70(3.69%)d86.02(47.32%)f87.82(48.31%)g 0.25(0.14%) (79.12%)0.8895*O22 s(1.56%)p62.80(98.21%)d 0.14(0.22%)
BD (3) U7 -O22	0.94910	(21.16%)0.4600*U7 s(6.47%)p 0.14(0.93%)d 6.88(44.56%)f 7.36(47.67%)g 0.06(0.37%) (78.84%)0.8879*O22 s(25.00%)p 2.99(74.74%)d 0.01(0.26%)
BD (1) U7 -O23	0.98983	(20.61%)0.4540*U7 s(0.04%)p79.95(3.11%)d99.99(48.13%)f99.99(48.61%)g 2.99(0.12%) (79.39%)0.8910*O23 s(0.39%)p99.99(99.38%)d 0.57(0.22%)
BD (2) U7 -O23	0.98285	(19.33%)0.4397*U7 s(0.00%)p 1.00(7.02%)d 5.89(41.33%)f 7.33(51.50%)g 0.02(0.15%) (80.67%)0.8982*O23 s(0.00%)p 1.00(99.78%)d 0.00(0.22%)
BD (3) U7 -O23	0.94398	(20.98%)0.4581*U7 s(8.23%)p 0.05(0.43%)d 5.24(43.09%)f 5.82(47.86%)g 0.05(0.39%) (79.02%)0.8889*O23 s(26.64%)p 2.74(73.10%)d 0.01(0.26%)



NBO analysis obtained at UB3PW91/6-31G(d,p) level (**Beta spin orbitals**).

Quintet

Donor Lewis-type NBO	Occupancy	Composition
BD (1) U7-O22	0.99355	(21.65%)0.4653*U7 s(0.05%)p24.17(1.21%)d99.99(42.65%)f99.99(56.01%)g 1.71(0.09%) (78.35%)0.8852*O22 s(3.17%)p30.46(96.60%)d 0.07(0.23%)
BD (2) U7-O22	0.99343	(20.39%)0.4516*U7 s(0.00%)p 1.00(0.62%)d78.46(49.02%)f80.43(50.26%)g 0.15(0.10%) (79.61%)0.8922*O22 s(0.00%)p 1.00(99.78%)d 0.00(0.22%)
BD (3) U7-O22	0.99234	(26.50%)0.5148*U7 s(0.04%)p 4.25(0.16%)d99.99(19.60%)f99.99(80.12%)g 2.12(0.08%) (73.50%)0.8573*O22 s(24.14%)p 3.13(75.60%)d 0.01(0.26%)
BD (1) U7-O23	0.99433	(20.30%)0.4506*U7 s(0.00%)p 1.00(0.73%)d66.92(48.71%)f69.34(50.47%)g 0.13(0.10%) (79.70%)0.8927*O23 s(0.00%)p 1.00(99.78%)d 0.00(0.22%)
BD (2) U7-O23	0.99365	(20.35%)0.4511*U7 s(0.02%)p35.35(0.70%)d99.99(49.17%)f99.99(50.01%)g 4.89(0.10%) (79.65%)0.8925*O23 s(1.97%)p49.76(97.81%)d 0.12(0.23%)

Figure S9. DFT-based NBO analysis for complex 6

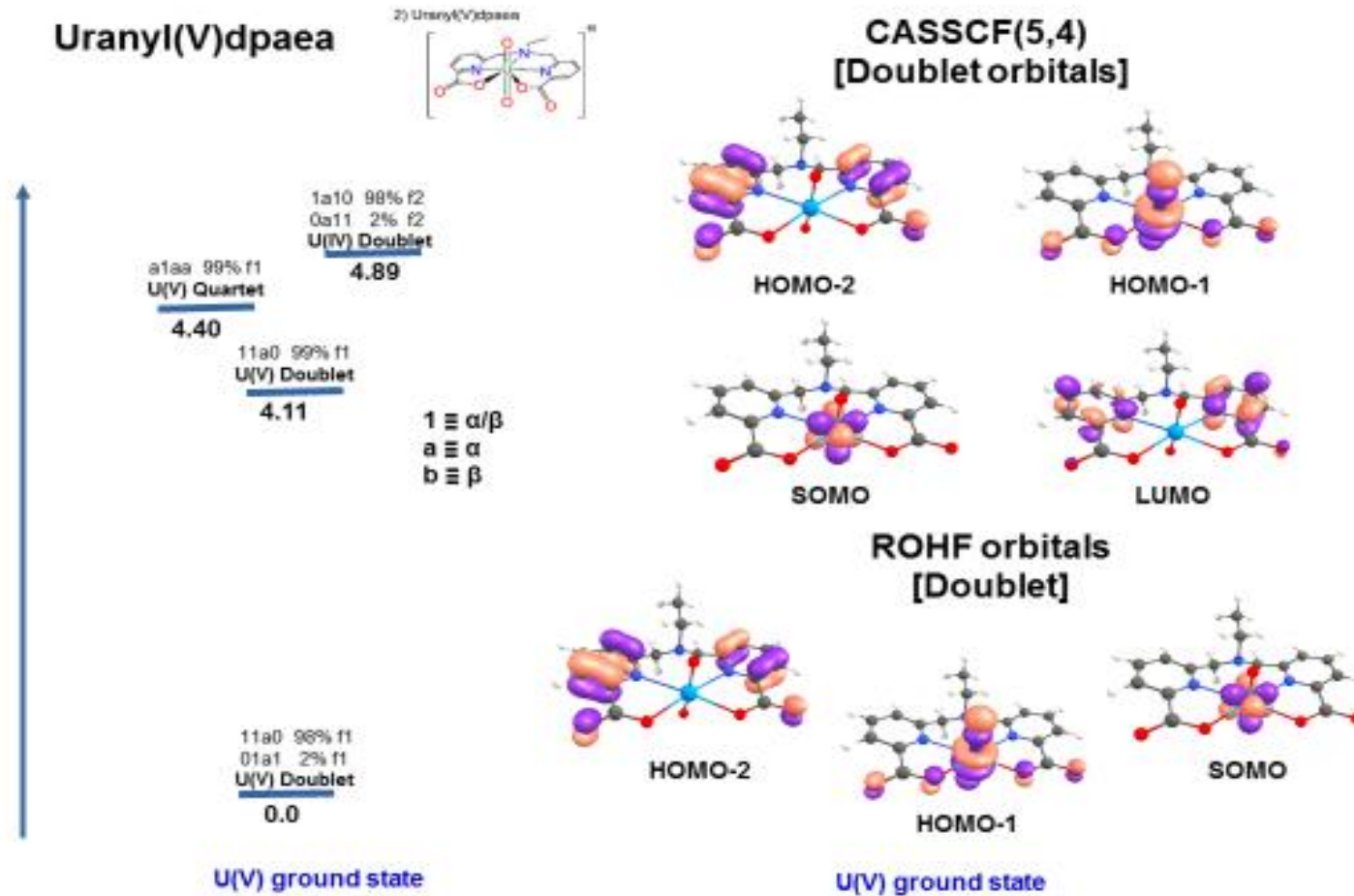


Figure S10. CASSCF computed energy spectrum and depiction of the chooses active orbitals for complex 7

Double

Natural charges obtained at UB3PWC9(1/6) level

Atom	Atom
C1	0.22329
N2	-0.43265
C3	0.16754
C4	-0.25526
C5	-0.21275
C6	-0.28443
U7	
O8	-0.65808
C9	0.81006
O10	-0.67878
C11	0.81001
O12	-0.65816
C13	-0.30108
N14	-0.48557
C15	-0.30071
C16	0.22361
N17	-0.43222
C18	0.16750
C19	-0.25524
C20	-0.21258
C21	-0.28448
	H22 -0.69651
	O23 -0.69703
	O24 -0.67868
	C25 -0.29498
	C26 -0.73048
	H27 0.27467
	H28 0.24299
	H29 0.24256
	H30 0.21985
	H31 0.27815
	H32 0.27783
	H33 0.21986
	H34 0.24253
	H35 0.24300
	H36 0.27472
	H37 0.27018
	H38 0.26975
	H39 0.25169
	H40 0.23001
	H41 0.23017

Quarte

Natural charges obtained at UB3PWC9(1/6) level

Atom	Atom
C1	0.22059
N2	-0.45207
C3	0.14815
C4	-0.25170
C5	-0.22663
C6	-0.29148
U7	
O8	-0.66487
C9	0.80960
O10	-0.67691
C11	0.80950
O12	-0.66504
C13	-0.30094
N14	-0.48588
C15	-0.30064
C16	0.22151
N17	-0.45041
C18	0.14901
C19	-0.25190
C20	-0.22506
C21	-0.29143
	O22 -0.60790
	O23 -0.60588
	O24 -0.67707
	C25 -0.29413
	C26 -0.73008
	H27 0.27173
	H28 0.24019
	H29 0.23988
	H30 0.21959
	H31 0.27316
	H32 0.27312
	H33 0.21965
	H34 0.24011
	H35 0.24046
	H36 0.27198
	H37 0.26760
	H38 0.26698
	H39 0.25070
	H40 0.23116
	H41 0.23150

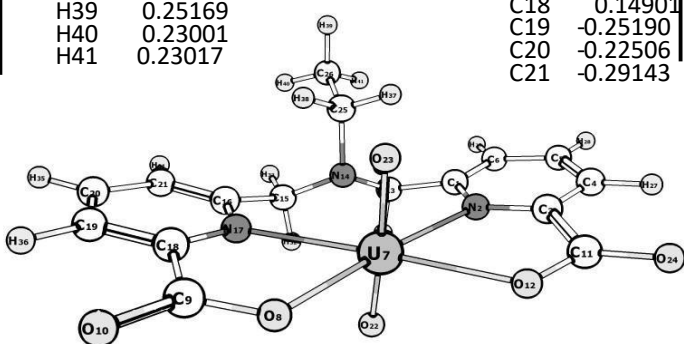


Figure S11. NPA Charges for complex 7

Molecular Orbital energy levels obtained at UB3PW91/6-31G(d,p) level (Energy in a.u.).

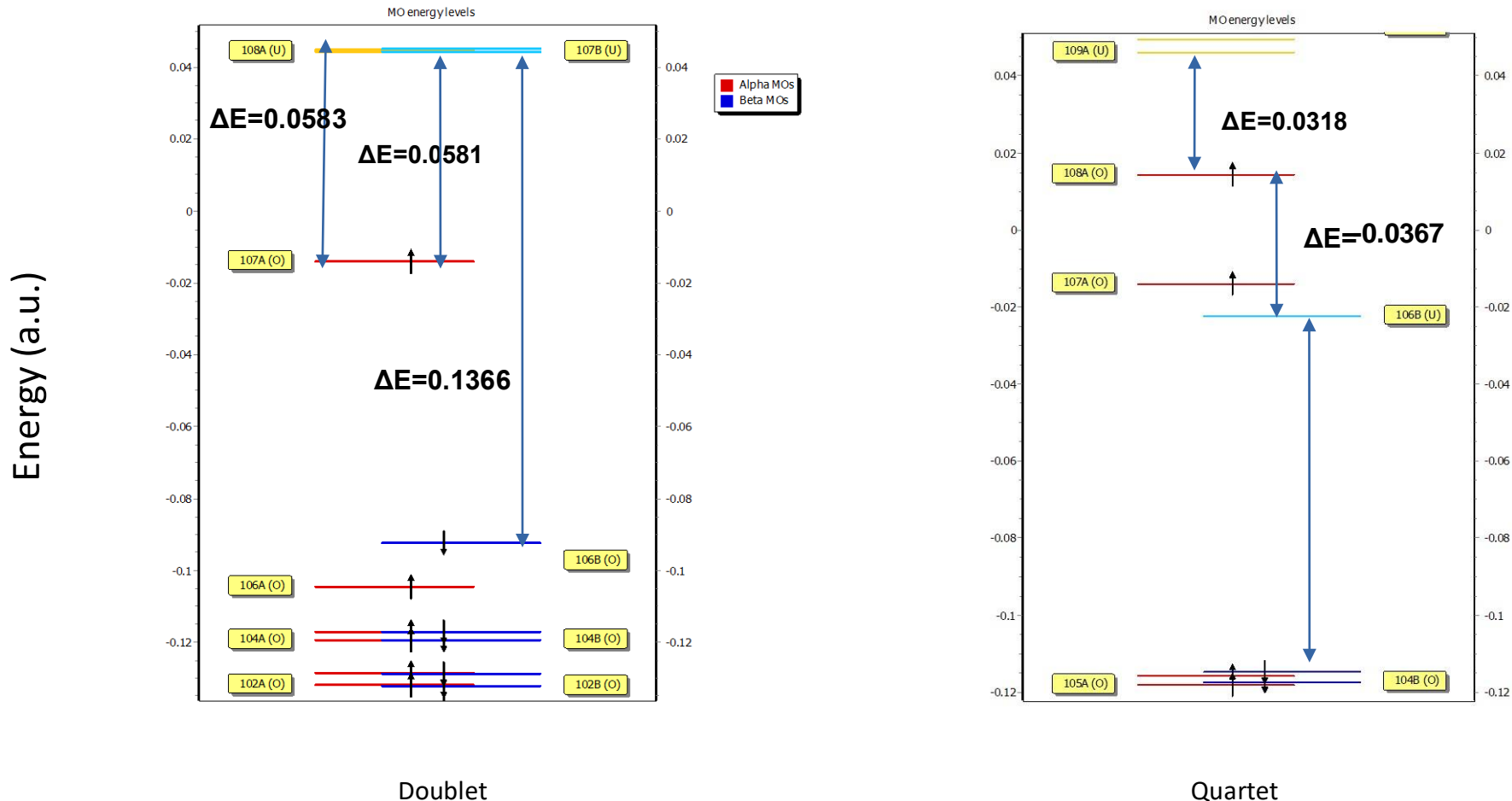


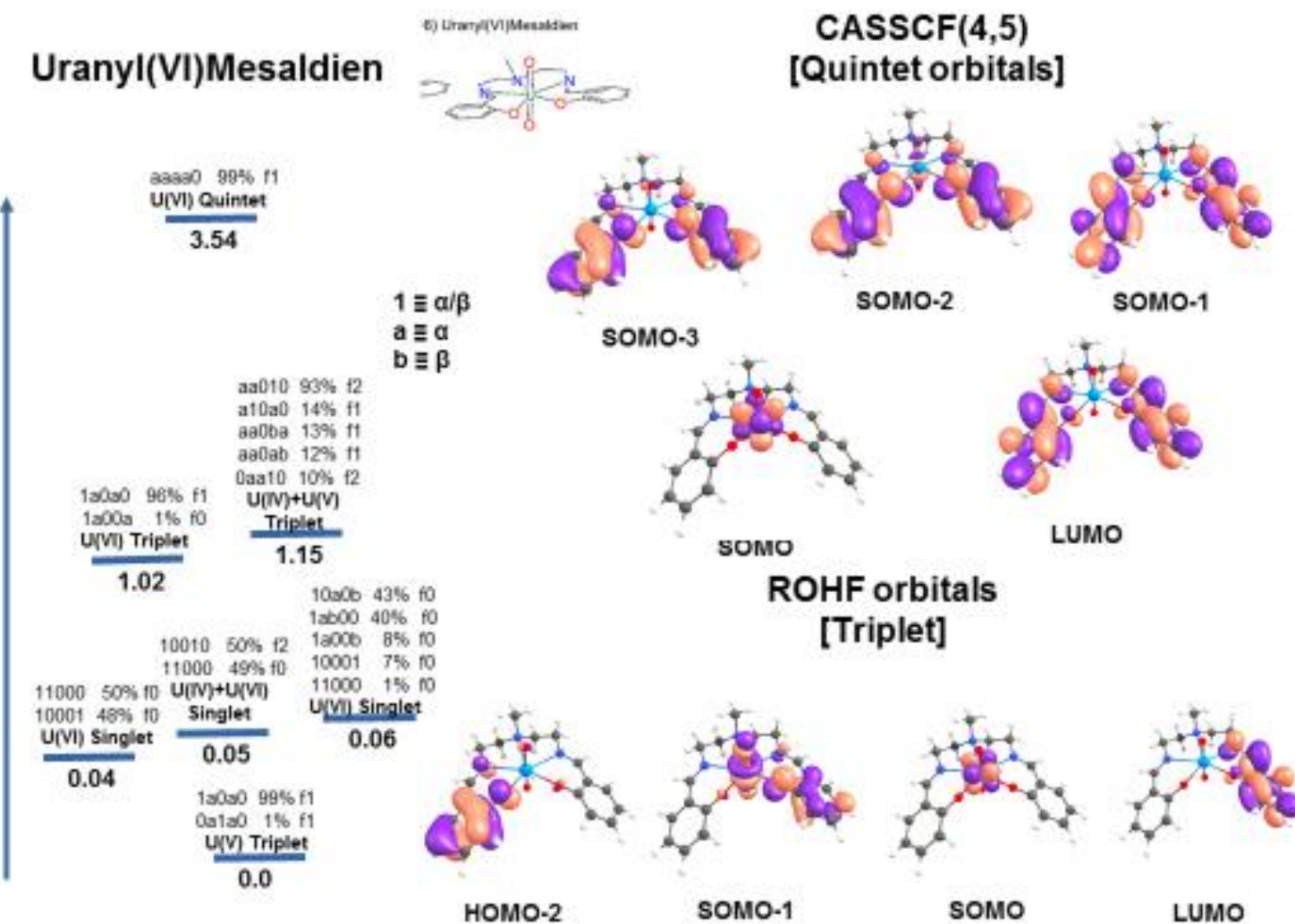
Figure S12. DFT computed energy spectrum for complex 7

NBO Analysis obtained at UB3PW91/6-31G(d,p) level (**alpha and beta spin orbitals**).

Doublet

Donor Lewis NBO	-type Occupancy	Composition	
(alpha spin) BD (1) U7 -O22	0.96343	(20.09%) 0.4482*U7 s(0.41%)p 5.19(2.14%)d99.99(44.59%)f99.99(52.59%)g 0.65(0.27%) (79.91%) 0.8939*O22 s(20.65%)p 3.83(79.16%)d 0.01(0.19%)	
BD (1) U7 -O23	0.96238	(20.31%) 0.4506*U7 s(0.42%)p 4.14(1.72%)d99.99(43.87%)f99.99(53.72%)g 0.64(0.27%) (79.69%) 0.8927*O23 s(22.52%)p 3.43(77.29%)d 0.01(0.19%)	
(beta spin) None BD orbital.			

Figure S13. DFT-based NBO analysis for complex 7



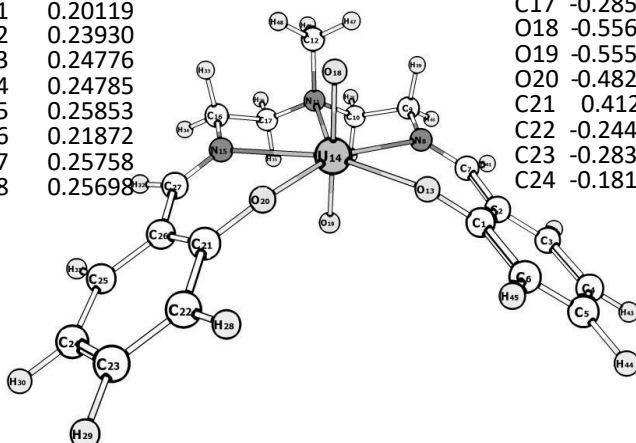
Figure

Figure S14. CASSCF computed energy spectrum and depiction of the chooses active orbitals for complex 1

Singlet

Natural charges obtained at UB3PW₉₆(f,p) level

Atom	Charge	Atom	Charge
C1	0.43643	C25	-0.19421
C2	-0.20728	C26	-0.20738
C3	-0.19422	C27	0.16534
C4	-0.29485	H28	0.25852
C5	-0.20572	H29	0.24784
C6	-0.29997	H30	0.24775
C7	0.16544	H31	0.23930
N8	-0.47370	H32	0.20123
C9	-0.28514	H33	0.24865
C10	-0.28848	H34	0.23868
N11	-0.49509	H35	0.26246
C12	-0.50507	H36	0.23648
O13	-0.60049	H37	0.26265
U14	1.46194	H38	0.23637
N15	-0.47361	H39	0.24883
C16	-0.28505	H40	0.23868
C17	-0.28846	H41	0.20119
O18	-0.53127	H42	0.23930
O19	-0.53013	H43	0.24776
O20	-0.60030	H44	0.24785
C21	0.43648	H45	0.25853
C22	-0.29995	H46	0.21872
C23	-0.20574	H47	0.25758
C24	-0.29486	H48	0.25698



Quintet

Natural charges obtained at UB3PW₉₆(f,p) level

Atom	Charge	Atom	Charge
C1	0.41224	C25	-0.25060
C2	-0.10251	C26	-0.10297
C3	-0.25102	C27	0.05475
C4	-0.18138	H28	0.26076
C5	-0.28429	H29	0.25055
C6	-0.24466	H30	0.25119
C7	0.05399	H31	0.24718
N8	-0.44216	H32	0.19451
C9	-0.28452	H33	0.24803
C10	-0.28577	H34	0.23304
N11	-0.49340	H35	0.26181
C12	-0.50394	H36	0.23059
O13	-0.48258	H37	0.26201
U14	1.21352	H38	0.23043
N15	-0.44173	H39	0.24813
C16	-0.28447	H40	0.23302
C17	-0.28572	H41	0.19440
O18	-0.55666	H42	0.24716
O19	-0.55577	H43	0.25114
O20	-0.48254	H44	0.25049
C21	0.41246	H45	0.26070
C22	-0.24481	H46	0.21255
C23	-0.28360	H47	0.25661
C24	-0.18199	H48	0.25584

Figure S15. NPA Charges for complex 1

Molecular Orbital energy levels obtained at UB3PW91/6-31G(d,p) level (Energy in a.u.).

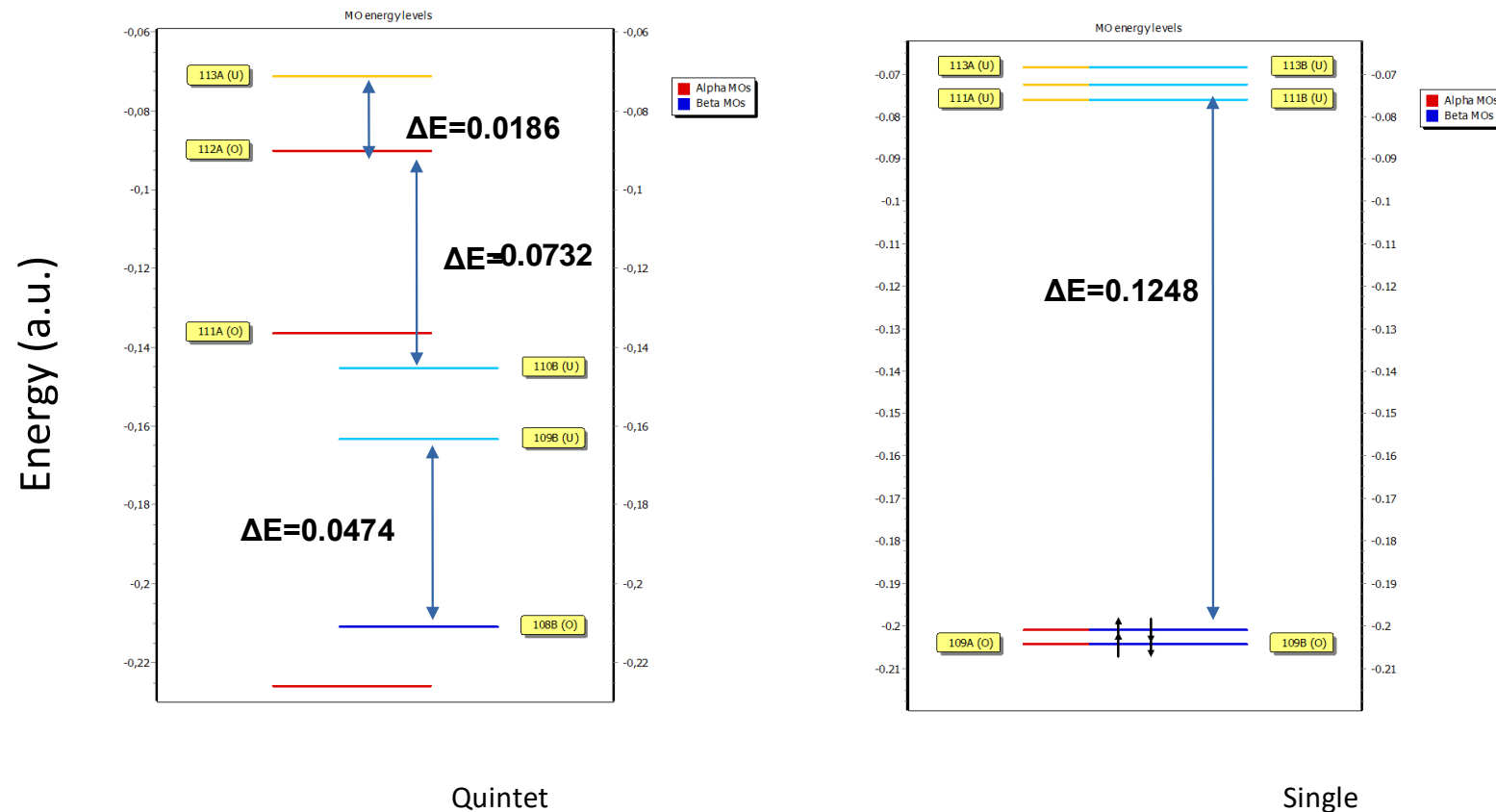
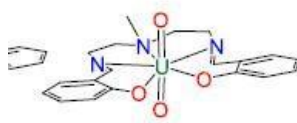


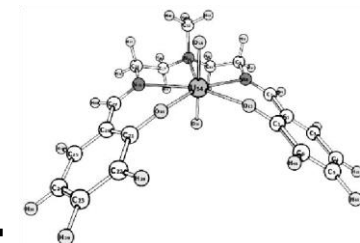
Figure S16. DFT computed energy spectrum for complex 1

6) Uranyl(VI)Mesaldien



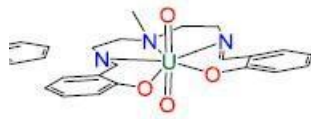
NBO Analysis obtained at UB3PW91/631G(d,p) level (**alpha and beta spin orbitals**)

Singlet



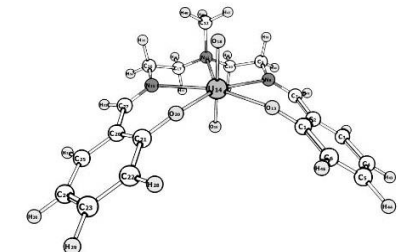
Donor Lewis-type NBO	Occupancy	Composition
(alpha spin) BD (1) U14-O18	0.99485	(21.01%) 0.4584* U14 s(0.00%)p 1.00(0.67%)d74.02(49.50%)f74.35(49.73%)g 0.15(0.10%) (78.99%) 0.8887* O18 s(0.00%)p 1.00(99.78%)d 0.00(0.22%)
BD (2) U14-O18	0.99035	(21.43%) 0.4630* U14 s(0.03%)p43.76(1.24%)d99.99(47.66%)f99.99(50.95%)g 4.34(0.12%) (78.57%) 0.8864* O18 s(1.10%)p90.08(98.68%)d 0.21(0.23%)
BD (3) U14-O18	0.96274	(22.90%) 0.4785* U14 s(0.18%)p 1.51(0.28%)d99.99(49.18%)f99.99(50.07%)g 1.59(0.29%) (77.10%) 0.8781* O18 s(25.46%)p 2.92(74.27%)d 0.01(0.27%)
BD (1) U14-O19	0.99464	(21.27%) 0.4612* U14 s(0.07%)p20.13(1.45%)d99.99(48.59%)f99.99(49.79%)g 1.36(0.10%) (78.73%) 0.8873* O19 s(0.01%)p 1.00(99.77%)d 0.00(0.22%)
BD (2) U14-O19	0.99469	(21.13%) 0.4597* U14 s(0.00%)p 1.00(0.74%)d64.23(47.48%)f69.93(51.69%)g 0.13(0.10%) (78.87%) 0.8881* O19 s(0.00%)p 1.00(99.78%)d 0.00(0.22%)
BD (3) U14-O19	0.95684	(22.67%) 0.4761* U14 s(0.15%)p 2.76(0.43%)d99.99(50.42%)f99.99(48.68%)g 2.07(0.32%) (77.33%) 0.8794* O19 s(27.07%)p 2.68(72.67%)d 0.01(0.26%)
(beta spin) BD (1) U14-O18	0.99485	(21.01%) 0.4584* U14 s(0.00%)p 1.00(0.67%)d74.02(49.50%)f74.35(49.73%)g 0.15(0.10%) (78.99%) 0.8887* O18 s(0.00%)p 1.00(99.78%)d 0.00(0.22%)
BD (2) U14-O18	0.99035	(21.43%) 0.4630* U14 s(0.03%)p43.76(1.24%)d99.99(47.66%)f99.99(50.95%)g 4.34(0.12%) (78.57%) 0.8864* O18 s(1.10%)p90.08(98.68%)d 0.21(0.23%)
BD (3) U14-O18	0.96274	(22.90%) 0.4785* U14 s(0.18%)p 1.51(0.28%)d99.99(49.18%)f99.99(50.07%)g 1.59(0.29%) (77.10%) 0.8781* O18 s(25.46%)p 2.92(74.27%)d 0.01(0.27%)
BD (1) U14-O19	0.99464	(21.27%) 0.4612* U14 s(0.07%)p20.13(1.45%)d99.99(48.59%)f99.99(49.79%)g 1.36(0.10%) (78.73%) 0.8873* O19 s(0.01%)p 1.00(99.77%)d 0.00(0.22%)
BD (2) U14-O19	0.99469	(21.13%) 0.4597* U14 s(0.00%)p 1.00(0.74%)d64.23(47.48%)f69.93(51.69%)g 0.13(0.10%) (78.87%) 0.8881* O19 s(0.00%)p 1.00(99.78%)d 0.00(0.22%)
BD (3) U14-O19	0.95684	(22.67%) 0.4761* U14 s(0.15%)p 2.76(0.43%)d99.99(50.42%)f99.99(48.68%)g 2.07(0.32%) (77.33%) 0.8794* O19 s(27.07%)p 2.68(72.67%)d 0.01(0.26%)

6) Uranyl(VI)Mesaldien



NBO analysis obtained at UB3PW91/6 -31G(d,p) level (**Alpha spin orbitals**).

Quintet



Donor Lewis -type NBO	Occupancy	Composition
(alpha spin) BD (1) U14 -O18	0.96336	(21.42%)0.4628* U14 s(0.34%)p 2.65(0.90%)d99.99(47.57%)f99.99(50.86%)g 0.97(0.33%) (78.58%)0.8865* O18 s(29.30%)p 2.41(70.48%)d 0.01(0.23%)
BD (1) U14 -O19	0.96305	(21.02%)0.4584* U14 s(0.24%)p 3.00(0.73%)d99.99(48.95%)f99.99(49.75%)g 1.39(0.34%) (78.98%)0.8887* O19 s(31.39%)p 2.18(68.39%)d 0.01(0.22%)
(beta spin) BD (1) U14 -O18	0.98190	(19.37%)0.4401* U14 s(0.00%)p 1.00(1.58%)d25.97(41.09%) f36.18(57.25%)g 0.05(0.07%) (80.63%) 0.8979* O18 s(0.00%)p 1.00(99.80%)d 0.00(0.20%)
BD (2) U14 -O18	0.86888	(18.18%)0.4264* U14 s(0.45%)p 7.03(3.14%)d93.95(41.99%)f99.99(54.16%)g 0.60(0.27%) (81.82%) 0.9045* O18 s(12.27%)p 7.13(87.48%)d 0.02(0.25%)
BD (1) U14 -O19	0.84612	(18.62%)0.4315* U14 s(1.37%)p 3.52(4.83%)d28.63(39.33%)f39.44(54.18%)g 0.21(0.29%) (81.38%)0.9021* O19 s(10.89%)p 8.16(88.86%)d 0.02(0.25%)

Figure S17. DFT-based NBO analysis for complex 1

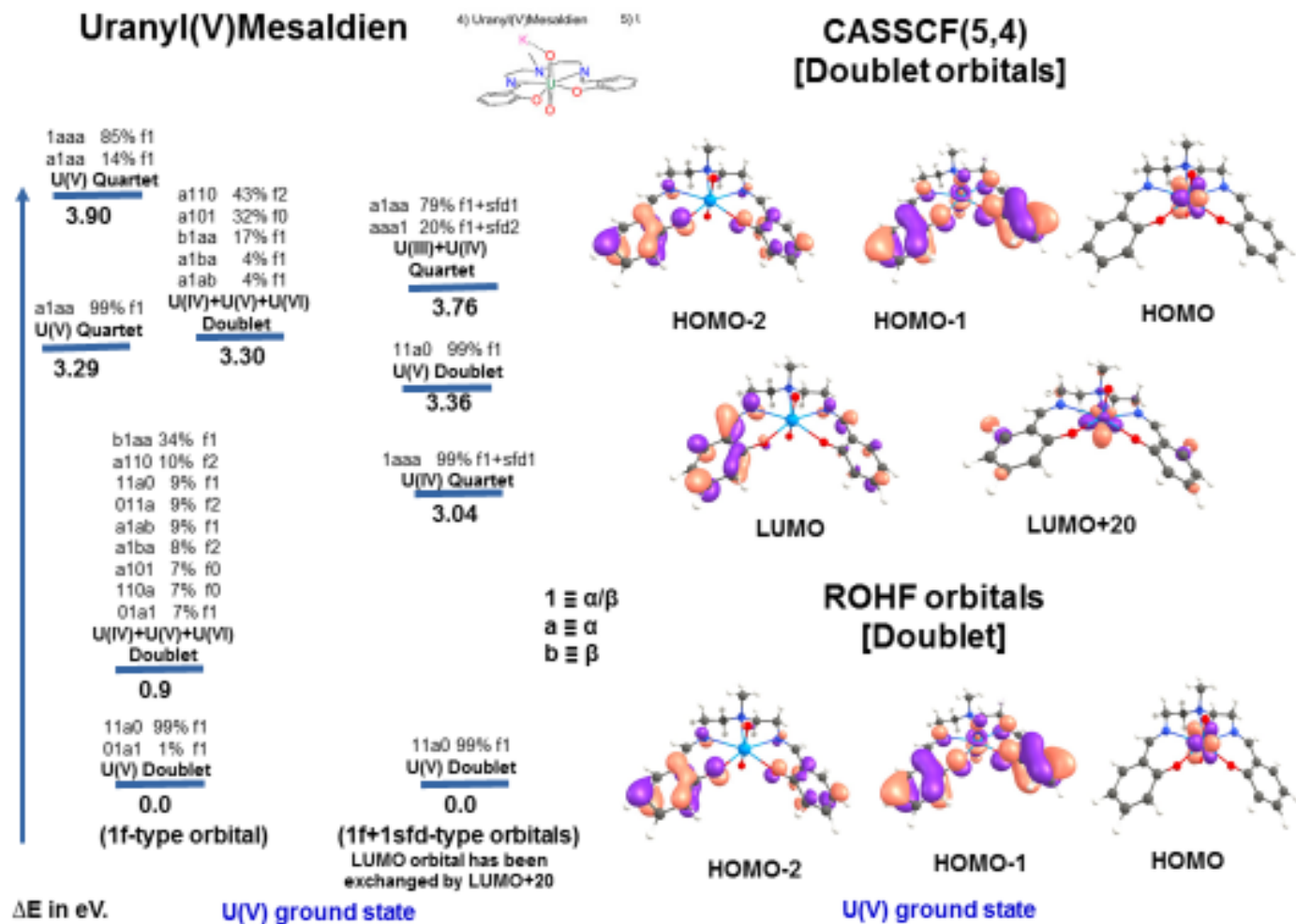


Figure S18. CASSCF computed energy spectrum and depiction of the chooses active orbitals for complex 2



Doublet

Natural charges obtained at UB3PW91/6-31G(d,p) level

Atom	Charge	Atom	Charge
C1	0.45586	C25	-0.20734
C2	-0.21874	C26	-0.21902
C3	-0.20723	C27	0.13464
C4	-0.32801	H29	0.24491
C5	-0.23375	H29	0.22816
C6	-0.31501	H30	0.22735
C7	0.13581	H31	0.22229
N8	-0.47216	H32	0.17505
C9	-0.27861	H33	0.23376
C10	-0.28546	H34	0.21980
N11	-0.49094	H35	0.26626
C12	-0.50013	H36	0.21314
O13	-0.61348	H37	0.26552
U14	1.32359	H38	0.21326
N15	-0.47357	H39	0.23439
C16	-0.27911	H40	0.21880
C17	-0.28574	H41	0.17500
O18	-0.68784	H42	0.22238
O19	-0.68821	H43	0.22741
O20	-0.61253	H44	0.22823
C21	0.45570	H45	0.24502
C22	-0.31527	H46	0.19591
C23	-0.23413	H47	0.25609
C24	-0.32824	H48	0.25717

Quartet

Natural charges obtained at UB3PW91/6-31G(d,p) level

Atom	Charge	Atom	Charge
C1	0.42462	C25	-0.25383
C2	-0.15778	C26	-0.15932
C3	-0.25484	C27	0.05084
C4	-0.25894	H28	0.24288
C5	-0.29209	H29	0.22695
C6	-0.29345	H30	0.22764
C7	0.04999	H31	0.22404
N8	-0.49621	H32	0.17243
C9	-0.27534	H33	0.22690
C10	-0.28468	H34	0.21904
N11	-0.49284	H35	0.26389
C12	-0.50015	H36	0.21191
O13	-0.56164	H37	0.26327
U14	1.33744	H38	0.21180
N15	-0.49708	H39	0.22741
C16	-0.27594	H40	0.21819
C17	-0.28501	H41	0.17215
O18	-0.64303	H42	0.22415
O19	-0.63508	H43	0.22767
O20	-0.56260	H44	0.22897
C21	0.42530	H45	0.24291
C22	-0.29447	H46	0.19803
C23	-0.29078	H47	0.25521
C24	-0.26189	H48	0.25618



Figure S19. NPA Charges for complex 2

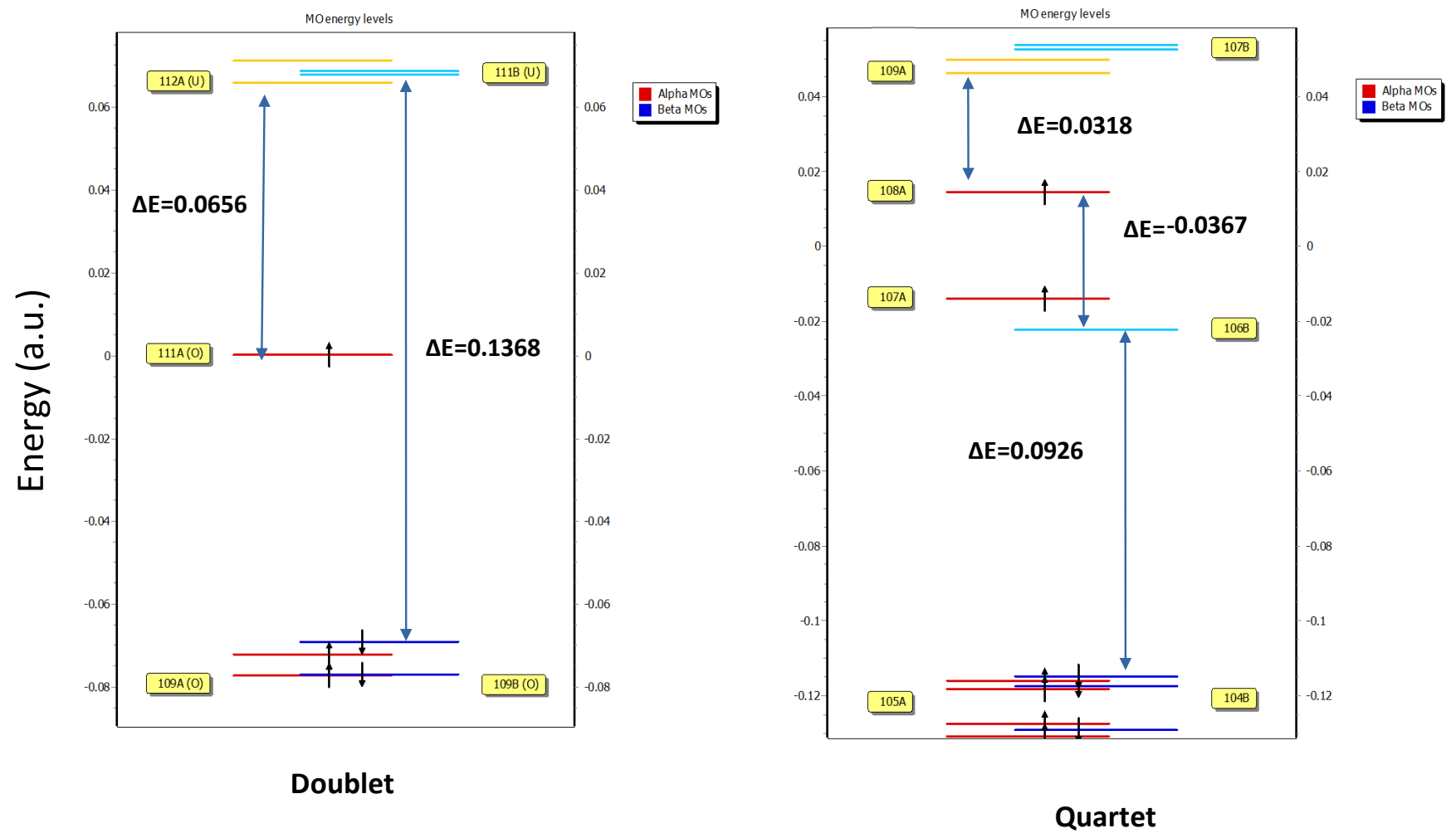
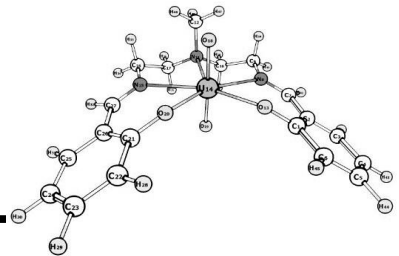


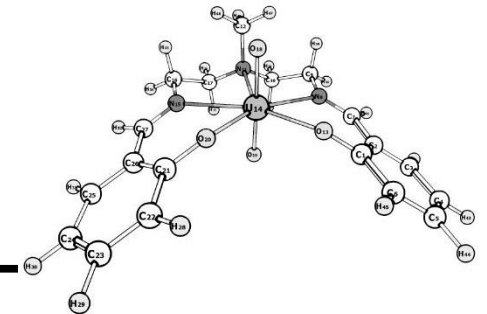
Figure S20. DFT computed energy spectrum for complex 2



(alpha spin orbitals)

Doublet

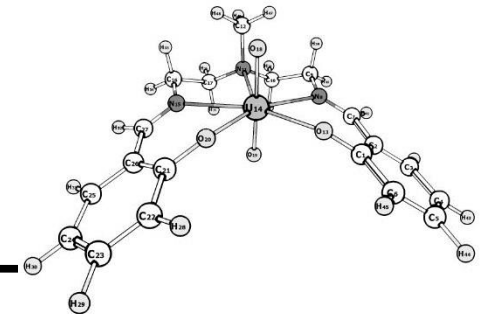
Donor Lewistype NBO	Occupancy	Composition
BD (1) N8-U14	0.96481	(91.16%)0.9548* N8 s(33.18%)p 2.01(66.78%)d 0.00(0.03% (8.84%)0.2974* U14 s(12.87%)p 2.50(32.15%)d 2.56(33.00%)f 1.71(21.98%)g 0.00(0.00%
BD (1) N11-U14	0.95266	(93.60%)0.9675* N11 s(19.43%)p 4.15(80.55%)d 0.00(0.02% (6.40%)0.2529* U14 s(11.37%)p 2.30(26.10%)d 4.03(45.81%)f 1.47(16.72%)g 0.00(0.01%
BD (1) O13-U14	0.98601	(90.59%)0.9518* O13 s(44.35%)p 1.25(55.64%)d 0.00(0.01% (9.41%)0.3067* U14 s(11.48%)p 2.15(24.72%)d 3.44(39.43%)f 2.12(24.35%)g 0.00(0.01%
BD (1) U14-N15	0.96513	(8.88%)0.2980* U14 s(13.07%)p 2.47(32.30%)d 2.51(32.86%)f 1.67(21.77%)g 0.00(0.00% (91.12%)0.9546* N15 s(33.37%)p 2.00(66.60%)d 0.00(0.03%
BD (1) U14O18	0.99313	(18.74%)0.4329* U14 s(0.00%)p 1.00(6.85%)d 7.39(50.64%)f 6.20(42.44%)g 0.01(0.07% (81.26%) 0.9015* O18 s(0.00%)p 1.00(99.82%)d 0.00(0.18%
BD (2) U14O18	0.99486	(24.91%)0.4991* U14 s(0.38%)p 4.64(1.74%)d 33.41(12.56%)f 99.99(85.25%)g 0.17(0.06% (75.09%)0.8665* O18 s(18.14%)p 4.50(81.66%)d 0.01(0.19%
BD (3) U14O18	0.99099	(19.77%) 0.4446* U14 s(0.42%)p 8.64(3.61%)d 99.99(45.96%)f 99.99(49.94%)g 0.18(0.08% (80.23%) 0.8957* O18 s(7.59%)p 12.16(92.22%)d 0.03(0.19%
BD (1) U14O19	0.99393	(18.70%) 0.4324* U14 s(0.00%)p 1.00(6.12%)d 8.01(48.99%)f 7.32(44.82%)g 0.01(0.07% (81.30%) 0.9017* O19 s(0.01%)p 1.00(99.82%)d 0.00(0.18%
	0.99231	(19.30%)0.4393* U14 s(0.00%)p 1.00(5.91%)d 8.41(49.75%)f 7.49(44.27%)g 0.01(0.07% (80.70%) 0.8983* O19 s(0.09%)p 99.99(99.73%)d 2.02(0.18%
	0.98620	(9.42%)0.3069* U14 s(11.60%)p 2.15(24.97%)d 3.39(39.27%)f 2.08(24.16%)g 0.00(0.01% (90.58%)0.9517* O20 s(44.56%)p 1.24(55.44%)d 0.00(0.01%



(beta spin orbitals).

Doublet

Donor Lewis -type NBO	Occupancy	Composition
BD (1) N8 -U14	0.96466	(91.42%) 0.9561* N8 s(33.37%)p 2.00(66.60%)d 0.00(0.03%) (8.58%) 0.2929* U14 s(12.93%)p 2.49(32.25%)d 2.56(33.14%)f 1.68(21.67%)g 0.00(0.00%)
BD (1) N11 -U14	0.95267	(93.86%) 0.9688* N11 s(19.50%)p 4.13(80.47%)d 0.00(0.02%) (6.14%) 0.2478* U14 s(11.76%)p 2.24(26.37%)d 3.93(46.20%)f 1.33(15.67%)g 0.00(0.01%)
BD (1) O13 -U14	0.98657	(90.77%) 0.9527* O13 s(45.93%)p 1.18(54.07%)d 0.00(0.01%) (9.23%) 0.3039* U14 s(11.59%)p 2.14(24.84%)d 3.36(38.96%)f 2.12(24.60%)g 0.00(0.01%)
BD (1) U14 -N15	0.96498	(8.62%) 0.2936* U14 s(13.16%)p 2.46(32.37%)d 2.51(32.96%)f 1.64(21.52%)g 0.00(0.00%) (91.38%) 0.9559* N15 s(33.55%)p 1.98(66.42%)d 0.00(0.03%)
BD (1) U14 -O18	0.99401	(17.63%) 0.4198* U14 s(0.00%)p 1.00(6.93%)d 7.22(50.02%)f 6.20(42.97%)g 0.01(0.08%) (82.37%) 0.9076* O18 s(0.00%)p 1.00(99.82%)d 0.00(0.18%)
BD (2) U14 -O18	0.99483	(22.60%) 0.4754* U14 s(0.41%)p 4.53(1.85%)d 43.01(17.60%)f 99.99(80.07%)g 0.17(0.07%) (77.40%) 0.8798* O18 s(17.61%)p 4.67(82.20%)d 0.01(0.19%)
BD (3) U14 -O18	0.99217	(18.74%) 0.4329* U14 s(0.53%)p 6.97(3.68%)d 78.76(41.51%)f 99.99(54.20%)g 0.16(0.08%) (81.26%) 0.9014* O18 s(10.42%)p 8.58(89.39%)d 0.02(0.19%)
BD (1) U14 -O19	0.99443	(17.57%) 0.4191* U14 s(0.00%)p 1.00(6.00%)d 8.04(48.24%)f 7.61(45.68%)g 0.01(0.08%) (82.43%) 0.9079* O19 s(0.01%)p 1.00(99.82%)d 0.00(0.18%)
	0.99325	(17.90%) 0.4230* U14 s(0.07%)p 90.45(6.08%)d 99.99(49.88%)f 99.99(43.90%)g 1.08(0.07%) (82.10%) 0.9061* O19 s(1.09%)p 90.94(98.73%)d 0.17(0.18%)
	0.98675	(9.24%) 0.3040* U14 s(11.71%)p 2.14(25.11%)d 3.31(38.77%)f 2.08(24.39%)g 0.00(0.01%) (90.76%) 0.9527* O20 s(46.13%)p 1.17(53.87%)d 0.00(0.01%)



(alpha spin orbitals).

Quartet

Donor Lewis -type NBO	Occupancy	Composition
BD (1) N8 -U14	0.96538	(90.45%)0.9511* N8 s(32.35%)p 2.09(67.62%)d 0.00(0.03%) (9.55%)0.3090* U14 s(13.22%)p 2.43(32.10%)d 2.49(32.96%)f 1.64(21.72%)g 0.00(0.00%)
BD (1) N11 -U14	0.95329	(93.21%)0.9654* N11 s(19.24%)p 4.20(80.74%)d 0.00(0.02%) (6.79%)0.2606* U14 s(11.63%)p 2.24(26.09%)d 3.96(46.03%)f 1.40(16.24%)g 0.00(0.01%)
BD (1) O13 -U14	0.98677	(90.70%)0.9524* O13 s(44.93%)p 1.23(55.06%)d 0.00(0.01%) (9.30%)0.3049* U14 s(11.44%)p 2.20(25.19%)d 3.39(38.82%)f 2.15(24.55%)g 0.00(0.01%)
BD (1) U14 -N15	0.96571	(9.57%)0.3094* U14 s(13.42%)p 2.40(32.22%)d 2.45(32.80%)f 1.61(21.56%)g 0.00(0.00%) (90.43%)0.9509* N15 s(32.54%)p 2.07(67.43%)d 0.00(0.03%)
BD (1) U14 -O18	0.99281	(18.47%)0.4298* U14 s(0.00%)p 1.00(6.66%)d 7.60(50.60%)f 6.41(42.67%)g 0.01(0.08%) (81.53%)0.9029* O18 s(0.01%)p 1.00(99.81%)d 0.00(0.18%)
BD (2) U14 -O18	0.99440	(19.49%)0.4415* U14 s(0.01%)p 99.99(4.70%)d 99.99(43.75%)f 99.99(51.48%)g 4.73(0.06%) (80.51%)0.8973* O18 s(0.72%)p 99.99(99.10%)d 0.25(0.18%)
BD (3) U14 -O18	0.99234	(24.62%)0.4961* U14 s(0.89%)p 0.36(0.32%)d 16.96(15.14%)f 93.63(83.56%)g 0.09(0.08%) (75.38%)0.8682* O18 s(26.14%)p 2.82(73.66%)d 0.01(0.20%)
BD (1) U14 -O19	0.99345	(18.44%)0.4294* U14 s(0.00%)p 1.00(5.86%)d 8.36(49.03%)f 7.68(45.03%)g 0.01(0.08%) (81.56%)0.9031* O19 s(0.00%)p 1.00(99.82%)d 0.00(0.18%)
	0.99362	(18.87%)0.4344* U14 s(0.00%)p 1.00(5.54%)d 8.93(49.45%)f 8.11(44.93%)g 0.01(0.07%) (81.13%)0.9007* O19 s(0.15%)p 99.99(99.67%)d 1.20(0.18%)
	0.98695	(9.31%)0.3052* U14 s(11.55%)p 2.20(25.45%)d 3.34(38.63%)f 2.11(24.36%)g 0.00(0.01%) (90.69%)0.9523* O20 s(45.17%)p 1.21(54.82%)d 0.00(0.01%)

NBO Analysis obtained at UB3PW91/6-31G(d,p) level (**beta spin orbitals**).

Quartet

Donor Lewis -type NBO	Occupancy	Composition
BD (1) U14 -O18	0.90572	(17.95%)0.4236* U14 s(0.45%)p 2.53(1.14%)d90.53(40.95%)f99.99(57.20%)g 0.56(0.25%) (82.05%)0.9058* O 18 s(13.56%)p 6.36(86.23%)d 0.02(0.21%)
BD (1) U14 -O19	0.89529	(18.44%)0.4295* U14 s(0.87%)p 2.04(1.78%)d42.78(37.35%)f68.44(59.74%)g 0.29(0.26%)(81.56%)0.9031* O19 s(12.91%)p 6.73(86.88%)d 0.02(0.21%)

Figure S21. DFT-based NBO analysis for complex 2

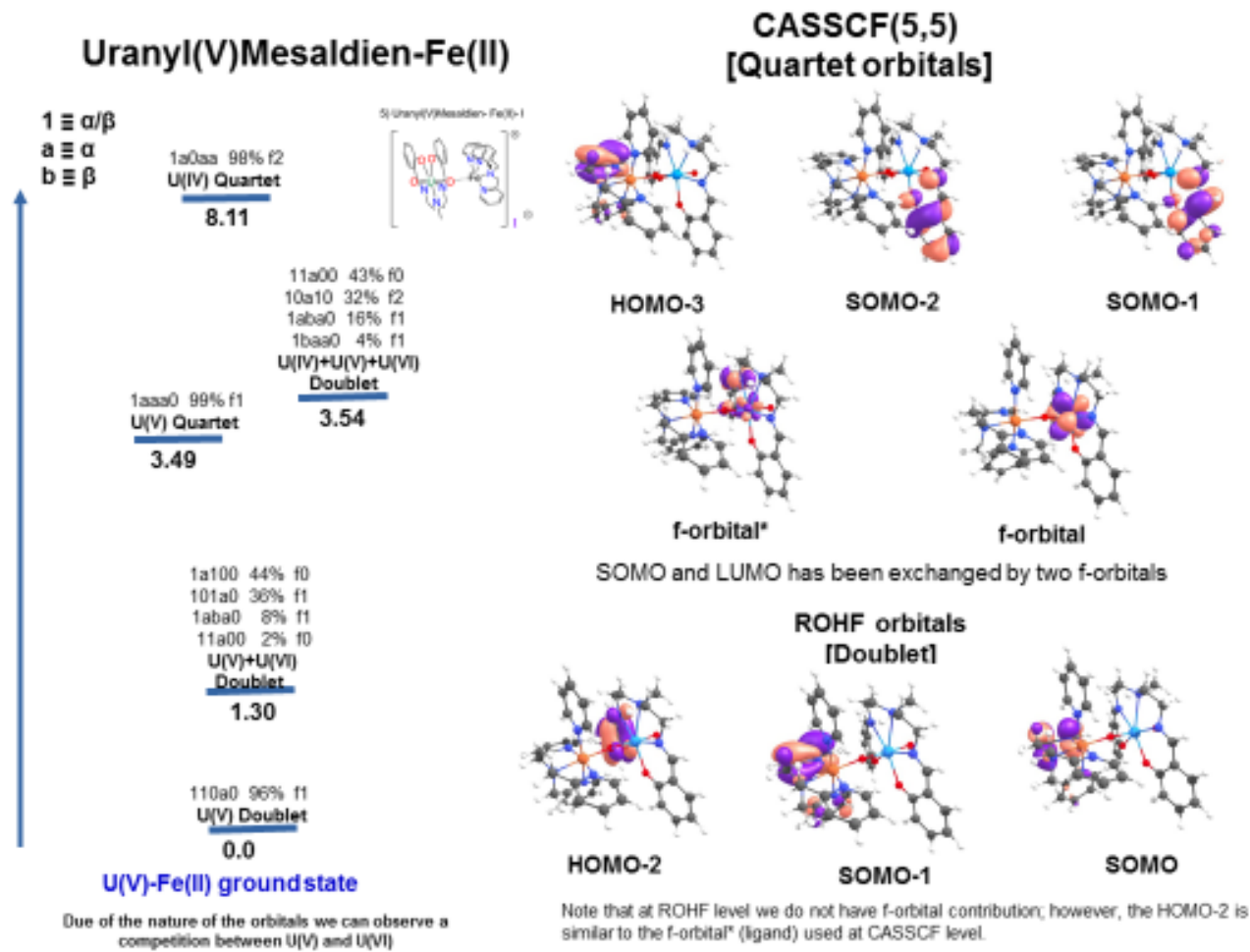


Figure S22. CASSCF computed energy spectrum and depiction of the chooses active orbitals for complex 3

Uranyl(V)Mesaldien-Fe(II)

Doublet

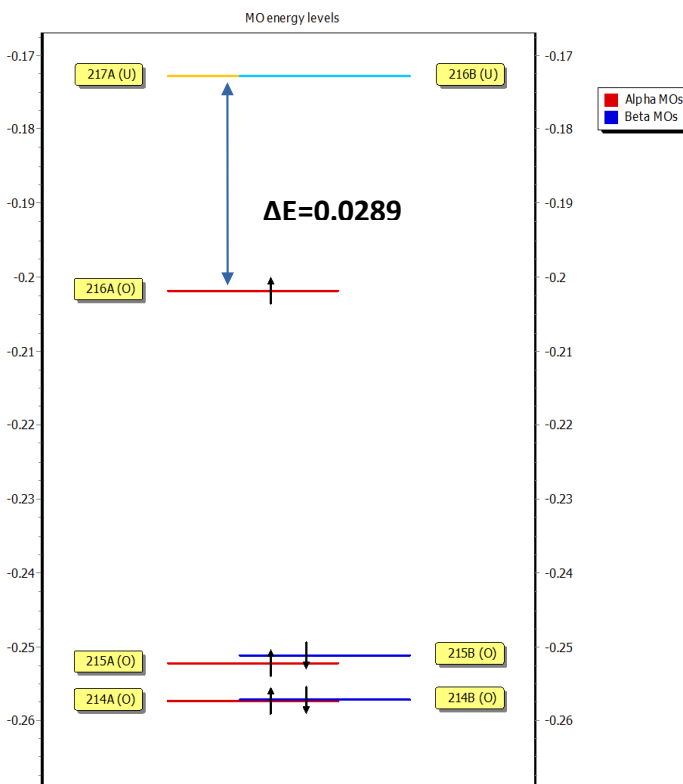
Natural charges obtained at UB3PW91/6-31G(d,p) level

Atom	Charge	Atom	Charge	Atom	Charge
U1	1.28571	C31	0.14896	H61	0.23991
Fe2	0.40099	H32	0.20791	H62	0.25119
O3	-0.63799	C33	-0.29781	C63	-0.22597
O4	-0.71224	H34	0.24399	C64	0.14336
O5	-0.62647	H35	0.24632	H65	0.20593
O6	-0.63787	C36	-0.25809	C66	-0.27380
N7	-0.49581	H37	0.27653	H67	0.27382
N8	-0.43785	C38	-0.19832	C68	0.18880
N9	-0.40140	H39	0.25280	C69	-0.30117
N10	-0.41190	C40	-0.19906	H70	0.25371
N11	-0.39950	H41	0.24110	C71	-0.18368
N12	-0.49627	C42	-0.25698	H72	0.27389
N13	-0.49149	H43	0.28425	C73	-0.30255
N14	-0.39082	C44	-0.18351	H74	0.25270
C15	-0.27402	H45	0.27032	C75	-0.28431
H16	0.23816	C46	0.19250	H76	0.26741
H17	0.23543	C47	0.07741	C77	-0.18078
C18	-0.31532	H48	0.27632	H78	0.27425
H19	0.25352	C49	-0.26850	C79	-0.25810
C20	0.44685	H50	0.26910	H80	0.28199
C21	-0.30110	C51	-0.29290	C81	-0.27094
H22	0.28096	H52	0.26340	H82	0.27362
H23	0.29055	H53	0.27345	C83	-0.50381
C24	-0.22012	C54	-0.18025	H84	0.26248
C25	0.01757	H55	0.27320	H85	0.21556
H26	0.25184	C56	-0.19290	H86	0.26237
C27	0.06519	H57	0.24214	C87	0.44569
H28	0.27831	C58	-0.20032	C88	0.17531
C29	-0.31807	H59	0.25224	C89	-0.28583
H30	0.25015	C60	-0.29335	H90	0.26405

Atom	Charge
C91	0.02450
H92	0.25479
C93	-0.29121
H94	0.27194
H95	0.26060
C96	0.05589
H97	0.27718
C98	-0.27580
H99	0.23355
H100	0.24303



Figure S23. NPA Charges for complex 3



Doublet

Figure S24. DFT computed energy spectrum for complex 3

NBO Analysis obtained at UB3PW91/6-31G(d,p) level (**alpha and beta spin orbitals**).

Doublet

Donor Lewis -type NBO	Occupancy	Composition
(alpha spin) BD (1) U1 -O6	0.99750	(20.31%)0.4506* U1 s(0.00%)p 1.00(1.45%)d26.93(39.16%)f40.80(59.33%)g 0.04(0.05%) (79.69%)0.8927* O 6 s(0.00%)p 1.00(99.78%)d 0.00(0.22%)
BD (2) U1 -O6	0.99623	(20.52%)0.4530* U1 s(0.04%)p31.46(1.38%)d99.99(40.83%)f99.99(57.70%)g 1.19(0.05%) (79.48%)0.8915* O6 s(0.05%)p99.99(99.73%)d 4.87(0.23%)
BD (3) U1 -O6	0.99375	(24.97%)0.4997* U1 s(0.05%)p 7.18(0.39%)d99.99(10.08%)f99.99(89.39%)g 1.36(0.07%) (75.03%)0.8662* O6 s(21.54%)p 3.63(78.18%)d 0.01(0.27%)
(beta spin) None BD orbital.		

Figure S25. DFT-based NBO analysis for complex **3**

Table S6. Cartesian coordinates of all optimized structures.

Uranyl(VI)dpaea

Singlet

C	8.909405	12.330373	4.502098
N	9.016863	11.993678	3.209937
C	9.570549	12.844275	2.336036
C	10.079959	14.078418	2.730655
C	10.001469	14.424980	4.074514
C	9.402762	13.543173	4.976381
U	8.393270	9.682360	2.277569
O	7.969495	7.795712	1.108028
C	7.798964	6.568990	1.509024
O	7.744386	5.559195	0.831835
C	9.570943	12.387093	0.887052
O	9.011809	11.220630	0.740758
C	8.138840	11.356111	5.354122
N	8.462593	9.954959	5.025341
C	7.443827	9.057857	5.602522
C	7.494718	7.678013	4.999994
N	7.693500	7.642116	3.675737
C	7.631648	6.477971	3.016367
C	7.395089	5.272211	3.670759
C	7.217277	5.294002	5.049237
C	7.261518	6.513544	5.727419
O	6.699992	10.199021	2.320443
O	10.080516	9.189750	2.467510
O	10.043581	13.105699	0.025958
C	9.841453	9.584417	5.456588
C	10.145319	9.660807	6.951657
H	10.515450	14.721128	1.973566
H	10.395010	15.375584	4.423197
H	9.313564	13.794627	6.028680
H	8.280920	11.578281	6.420724
H	7.073891	11.503247	5.135495
H	6.462055	9.483227	5.360492
H	7.508811	9.003937	6.697900
H	7.110564	6.561714	6.801389
H	7.038386	4.373158	5.597072
H	7.356405	4.364511	3.078760
H	10.528833	10.229229	4.903412
H	10.024225	8.571875	5.088624
H	11.185140	9.357371	7.105703

H	9.524692	8.987850	7.550901
H	10.044815	10.671826	7.357076

Uranyl(V)dpaea

Doublet

C	8.909458	12.332108	4.494400
N	9.002789	12.029446	3.193233
C	9.584527	12.886306	2.346257
C	10.137459	14.090125	2.786717
C	10.076446	14.398197	4.139941
C	9.446166	13.508694	5.012869
U	8.342428	9.689857	2.201409
O	7.879669	7.638857	1.023772
C	7.746128	6.465515	1.509106
O	7.683542	5.382455	0.922813
C	9.580582	12.502235	0.863899
O	9.013567	11.383845	0.623046
C	8.104364	11.361106	5.321896
N	8.435417	9.962994	5.027457
C	7.410996	9.065645	5.571508
C	7.492433	7.674430	4.993009
N	7.661679	7.617487	3.665925
C	7.621182	6.438289	3.035153
C	7.437641	5.241676	3.730336
C	7.293671	5.286281	5.111278
C	7.315048	6.523602	5.758422
O	6.603822	10.222551	2.297791
O	10.075216	9.185918	2.407080
O	10.091188	13.302328	0.076640
C	9.807610	9.592597	5.434429
C	10.124545	9.668036	6.929953
H	10.592481	14.735196	2.043077
H	10.506895	15.322254	4.519092
H	9.366291	13.723746	6.074960
H	8.197394	11.606619	6.393102
H	7.051499	11.499559	5.045538
H	6.439315	9.480641	5.275327
H	7.424585	9.019803	6.673356
H	7.191412	6.597686	6.835405
H	7.159827	4.372263	5.685356
H	7.414963	4.324079	3.152701
H	10.489500	10.232573	4.869341

H	9.987814	8.583422	5.056620
H	11.166397	9.369602	7.086017
H	9.502277	8.994704	7.529129
H	10.014280	10.680199	7.333169

Uranyl(VI)Mesaldien

Triplet

C	2.812958	7.446767	12.408204
C	1.999638	6.319104	12.084712
C	2.089679	5.148570	12.867564
C	2.938228	5.070626	13.954852
C	3.738271	6.182108	14.269558
C	3.686840	7.339943	13.514398
C	1.120065	6.300942	10.946367
N	0.822263	7.275678	10.151263
C	-0.057051	6.963709	9.037898
C	-1.133662	8.030157	8.900242
N	-0.565459	9.374799	8.686939
C	0.040311	9.466042	7.347201
O	2.784906	8.533437	11.690317
U	1.312818	9.813038	10.618670
N	-0.148007	11.917278	10.042939
C	-1.067967	11.801909	8.924441
C	-1.626181	10.388673	8.839762
O	2.385168	10.003299	9.217679
O	0.088306	9.587396	11.882953
O	2.142736	11.624936	11.609473
C	1.730321	12.664936	12.276367
C	2.485891	13.167712	13.360383
C	2.066326	14.283880	14.061314
C	0.886981	14.963267	13.711615
C	0.143346	14.498526	12.644254
C	0.533223	13.354052	11.916423
C	-0.272962	12.964783	10.790326
H	3.400172	12.644660	13.622200
H	2.663990	14.642389	14.896033
H	0.569918	15.840006	14.267118
H	-0.768505	15.015300	12.349638
H	-1.080338	13.672661	10.550981
H	-0.538941	12.059817	7.998023

H	-1.909040	12.506676	9.010839
H	-2.163228	10.170297	9.768367
H	-2.347668	10.322076	8.007518
H	-1.715660	8.058517	9.826958
H	-1.818613	7.764612	8.076910
H	0.537755	6.900426	8.117775
H	-0.545668	5.985202	9.162368
H	0.667344	5.318528	10.745419
H	1.467389	4.296042	12.600714
H	2.990376	4.166519	14.552888
H	4.414039	6.132694	15.120107
H	4.308814	8.197869	13.749260
H	-0.709888	9.275524	6.562733
H	0.855666	8.750101	7.250296
H	0.478772	10.451639	7.195673

Uranyl(V)Mesaldien

Doublet

C	2.796852	7.238475	12.520720
C	2.065628	6.101179	12.018483
C	2.236749	4.836907	12.624327
C	3.086064	4.639621	13.695239
C	3.807476	5.745599	14.189976
C	3.674015	6.995570	13.624908
C	1.175504	6.174584	10.892943
N	0.843765	7.205607	10.185327
C	-0.043497	6.949902	9.070446
C	-1.120648	8.022630	8.969499
N	-0.572297	9.370735	8.774851
C	0.074251	9.501665	7.467988
O	2.698850	8.406600	12.014262
U	1.231609	9.797024	10.800465
N	-0.183314	11.973957	10.104359
C	-1.111195	11.797203	9.005944
C	-1.635873	10.368184	8.950647
O	2.448969	10.038572	9.472057
O	-0.125002	9.518342	11.979820
O	1.988269	11.702133	11.964206
C	1.628794	12.849559	12.393013
C	2.344595	13.486341	13.456071
C	1.985338	14.726641	13.937797
C	0.890940	15.431731	13.395645
C	0.181883	14.848862	12.364099
C	0.513236	13.579072	11.841572

C	-0.282926	13.091351	10.749959
H	3.186700	12.939729	13.871362
H	2.557516	15.168734	14.752502
H	0.613850	16.409309	13.780440
H	-0.666386	15.376418	11.926404
H	-1.074166	13.795063	10.436779
H	-0.611161	12.047868	8.059196
H	-1.979201	12.475254	9.082972
H	-2.132101	10.148691	9.901262
H	-2.385836	10.284820	8.139613
H	-1.680659	8.032634	9.909914
H	-1.821297	7.764844	8.151196
H	0.539897	6.916386	8.139096
H	-0.544941	5.969532	9.154401
H	0.739327	5.199038	10.614128
H	1.671027	3.996042	12.221267
H	3.196890	3.657061	14.145583
H	4.482320	5.611102	15.034410
H	4.227622	7.850235	14.003629
H	-0.646082	9.346095	6.642897
H	0.889877	8.784612	7.381322
H	0.532444	10.485610	7.374935

Uranyl(V)Mesaldien-Fe(II)

Doublet

U	6.951129	10.536040	35.862495
Fe	5.883785	9.562169	32.198044
O	8.000127	12.368289	34.993073
O	6.332853	10.050378	34.130823
O	8.857693	9.343165	35.483067
O	7.516917	11.023465	37.511128
N	5.321910	12.522421	35.888663
N	5.548485	9.010206	30.249820
N	6.281028	7.653990	32.386445
N	5.446241	11.395953	31.545265
N	3.908066	9.228183	32.761488
N	4.549279	10.091106	37.061764
N	6.661945	8.156333	36.837910
N	7.688390	10.099700	31.480081
C	4.268172	8.655451	37.017348
H	4.079138	8.389245	35.973368
H	3.350816	8.417585	37.593267
C	10.908568	8.177200	35.439482
H	11.333088	8.997777	34.866187

C	8.037822	13.663432	35.072551
C	6.854368	8.963170	29.552370
H	6.731787	9.078545	28.464509
H	7.226469	7.938017	29.744383
C	6.870618	14.420201	35.469179
C	2.946958	10.187199	32.646513
H	3.293613	11.128415	32.232992
C	7.092448	7.057207	33.287824
H	7.450398	7.704641	34.081152
C	9.216239	14.376873	34.754301
H	10.083126	13.786798	34.466467
C	5.628010	13.812770	35.797151
H	4.818924	14.534398	35.993064
C	3.912639	12.302664	36.150704
H	3.277296	12.723895	35.351268
H	3.595625	12.814593	37.080194
C	9.605043	11.546575	31.426605
H	10.295575	12.162170	31.992791
C	9.279240	15.764907	34.808500
H	10.209085	16.275300	34.560855
C	9.768586	6.100502	36.893306
H	9.314799	5.289075	37.464985
C	7.445599	5.722378	33.224469
H	8.100903	5.317927	33.988594
C	9.703450	11.416282	30.026802
H	10.475945	11.938150	29.466875
C	7.785093	9.967036	30.120019
C	8.590996	10.883013	32.099200
H	8.471459	10.993763	33.170189
C	6.152822	5.538539	31.203099
H	5.771053	4.980277	30.348924
C	4.960543	7.647402	30.374741
H	4.873747	7.127810	29.405933
H	3.949106	7.829576	30.768461
C	5.465064	13.763684	30.012644
H	5.480054	14.678745	29.425882
C	6.972631	15.838013	35.496073
H	6.086268	16.405711	35.784344
C	11.671022	7.064989	35.775836
H	12.713869	7.009852	35.466126
C	5.432752	7.831653	37.531062
H	5.161866	6.765806	37.412183
H	5.543348	7.985935	38.620576
C	8.955895	7.224088	36.578738
C	7.604038	7.237707	37.019666

H	7.319989	6.338555	37.589573
C	2.207171	7.811207	33.753304
H	1.978365	6.852499	34.214111
C	5.110795	11.384770	30.201719
C	8.141315	16.506353	35.179405
H	8.178536	17.594088	35.217287
C	6.954614	4.927432	32.156682
H	7.216722	3.875582	32.073302
C	11.094470	6.010646	36.510454
H	11.683891	5.134089	36.775152
C	5.116830	12.551586	29.434832
H	4.844082	12.490069	28.381633
C	1.210847	8.777264	33.560752
H	0.174984	8.591765	33.830144
C	5.832139	13.766327	31.384834
H	6.132799	14.675748	31.894735
C	1.628603	10.012474	33.020948
H	0.933405	10.839534	32.897319
C	4.581757	10.594732	38.432754
H	5.322136	10.041998	39.011139
H	3.589597	10.503983	38.917768
H	4.901690	11.636813	38.429943
C	9.550867	8.301226	35.818333
C	5.822872	6.890306	31.325953
C	8.771973	10.618866	29.379045
H	8.797076	10.485803	28.298800
C	3.512188	8.063948	33.363139
H	4.295698	7.331209	33.513324
C	4.645631	10.055258	29.716417
H	3.656740	9.789056	30.127363
H	4.578760	10.025496	28.616177
C	5.817896	12.579572	32.088756
H	6.112221	12.534077	33.133069
C	3.585475	10.822396	36.235262
H	2.554163	10.690106	36.618518
H	3.625488	10.387712	35.233636

7. X-ray absorption spectroscopy

U L₃ edge XANES and EXAFS of complexes 1 – 3

The U L₃ edge XAFS was measured at the INE beamline for actinide research at the Karlsruhe Research Accelerator (KARA), Karlsruhe, Germany.¹¹ The incident energy was monochromatized by a Ge(422) double crystal monochromator (DCM). The DCM was calibrated using the first inflection point of the Y K edge spectrum of an Y metal foil. The data was acquired in transmission mode using two Ar filled ionization chambers. Raw data were processed using Artemis and Athena, part of the Demeter software package, and scattering paths were generated using FEFF6.¹² EXAFS were fit in R space using a shell by shell approach (in the order Oyl, Oeq, N, C) (Figure S27, Table S7). Scattering paths were generated from crystallographic information files of compounds **1**, **2** and **3**. Shells with very similar distances (<0.01 Å) and the same backscattering atoms were grouped together to minimize fitting parameters. For each shell Debye-Waller factors and interatomic distances were fit, while coordination numbers were maintained constant according to the crystallographic structures. EXAFS were fit in the range of 3–12 Å⁻¹ in $\chi(k)$ and 1.13–3.7 Å in R space. The amplitude reduction factor was set to 0.95. The inclusion of C backscattering paths was found to significantly improve the statistical fitting for all 3 complexes, corresponding to the peak at 3 Å in Figure S27 (right). This is consistent with the structures of the complexes. Deviations in bond lengths from crystallographic data were < 0.1 Å, and total Oyl, Oeq and N coordination numbers were the same for both EXAFS fits and crystallographic data.

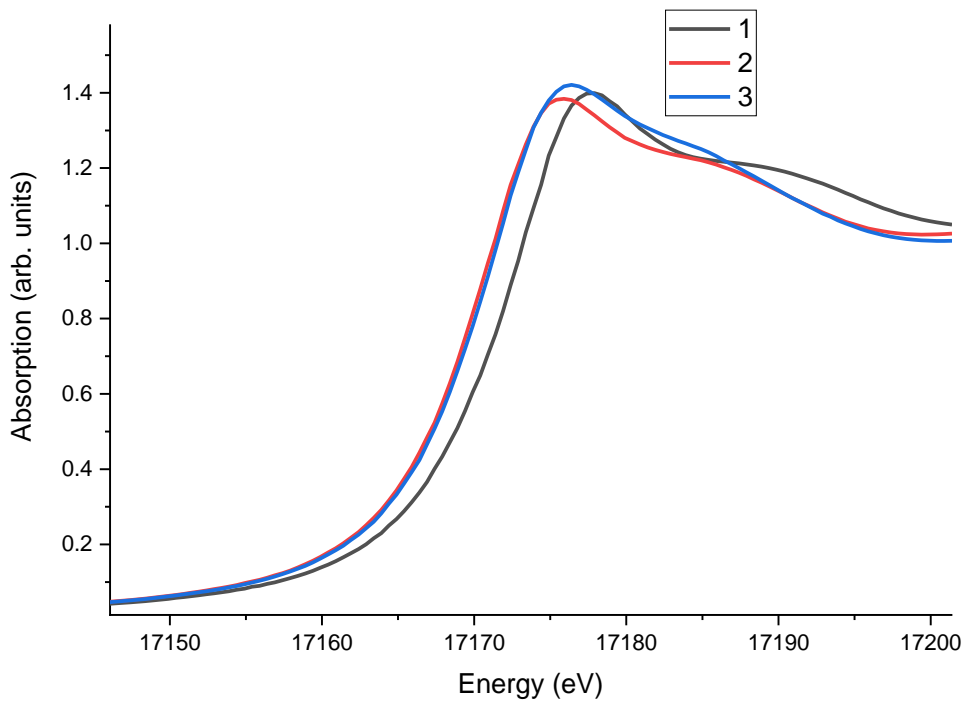


Figure S26. U L₃ edge XANES spectra of complexes **1**, **2** and **3**.

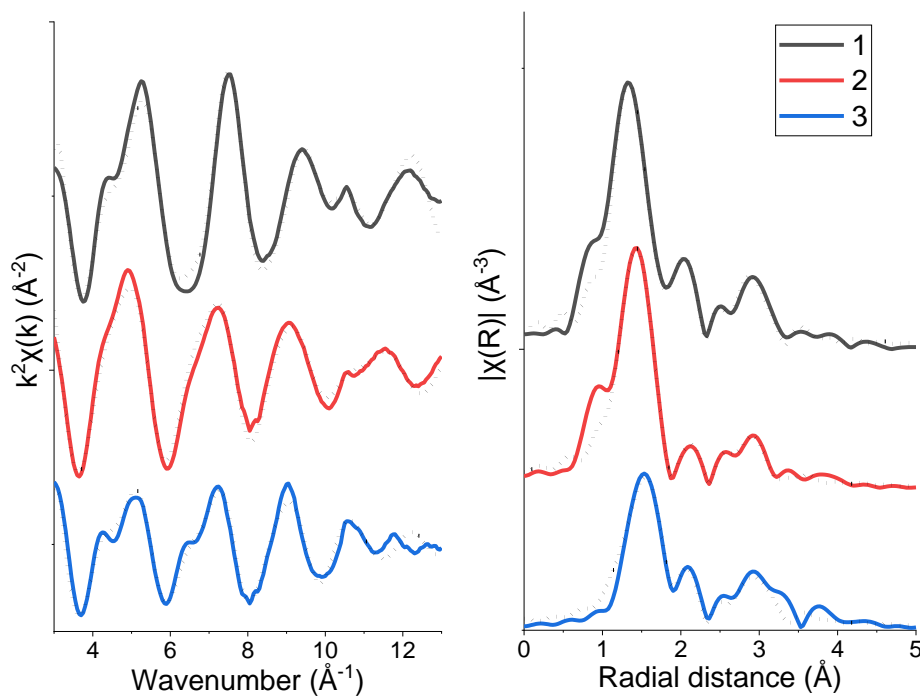


Figure S27. UL₃ edge EXAFS (left) and Fourier transformed EXAFS (right) of complexes 1, 2 and 3 with fits (dashed black lines).

Table S7. EXAFS fitting parameters and bond lengths from crystallographic data (cry)

Complex	path	N	R (Å)	σ^2 (Å ⁻²)	ΔE_0 (eV)	S ₀	R
1	O _{yl}	2	1.78(1)	0.0017(5)	1.5(18)	0.95	0.0068
	O _{eq}	2	2.25(1)	0.0013(7)			
	N1	2	2.57(2)	0.0082(20) ^a			
	N2	1	2.60(2)	0.0082(20) ^a			
	C1	3	3.48(5)	0.0068(20) ^b			
	C2	6	3.54(2)	0.0068(20) ^b			
1 (cry)	O _{yl}	1	1.779(3)				
	O _{yl}	1	1.784(3)				
	O _{eq}	2	2.218(3)				
	N1	1	2.578(4)				
	N2	1	2.604(4)				
	N3	1	2.609(4)				
2	O _{yl}	2	1.86(1)	0.0025(4)	2.0(18)	0.95	0.0032

	O _{eq}	2	2.32(1)	0.0044(10)	4.2(15)		
	N1	2	2.58(2)	0.0071(14) ^a	4.2(15)		
	N2	1	2.61(2)	0.0071(14) ^a	4.2(15)		
	C1	6	3.49(5)	0.0075(60) ^b	4.2(15)		
	C2	3	3.61(10)	0.0075(60) ^b	4.2(15)		
2 (cry)	O _{yl}	1	1.79(2)				
	O _{yl}	1	1.86(2)				
	O _{eq}	1	2.318(19)				
	O _{eq}	1	2.398(15)				
	N1	1	2.57(2)				
	N2	1	2.63(2)				
	N3	1	2.65(3)				
3	O _{yl}	2	1.92(1)	0.0068(18)	8.5(60)	0.95	0.0288
	O _{eq}	2	2.28(1)	0.0023(16)	8.0(1)		
	N1	2	2.58(2)	0.0096(57) ^a	8.0(1)		
	N2	1	2.61(2)	0.0096(57) ^a	8.0(1)		
	C1	3	3.56(5)	0.0101(47) ^b	8.0(1)		
	C2	6	3.58(10)	0.0101(47) ^b	8.0(1)		
3 (cry)	O _{yl}	1	1.84(2)				
	O _{yl}	1	1.935(19)				
	O _{eq}	1	2.26(2)				
	O _{eq}	1	2.29(2)				
	N1	1	2.58(3)				
	N2	1	2.59(3)				
	N3	1	2.62(3)				

Coordination number (N), U bond distances (R), Debeye-Waller factors (σ^2), shift in energy from calculated Fermi level (ΔE_0) and ‘goodness of fit’ factor (R). ^{a,b} denote tied Debeye-Waller factors. Numbers in parentheses are the standard deviation on the last decimal place.

U M_{4,5} edge HR-XANES experiments and FDMNES computations

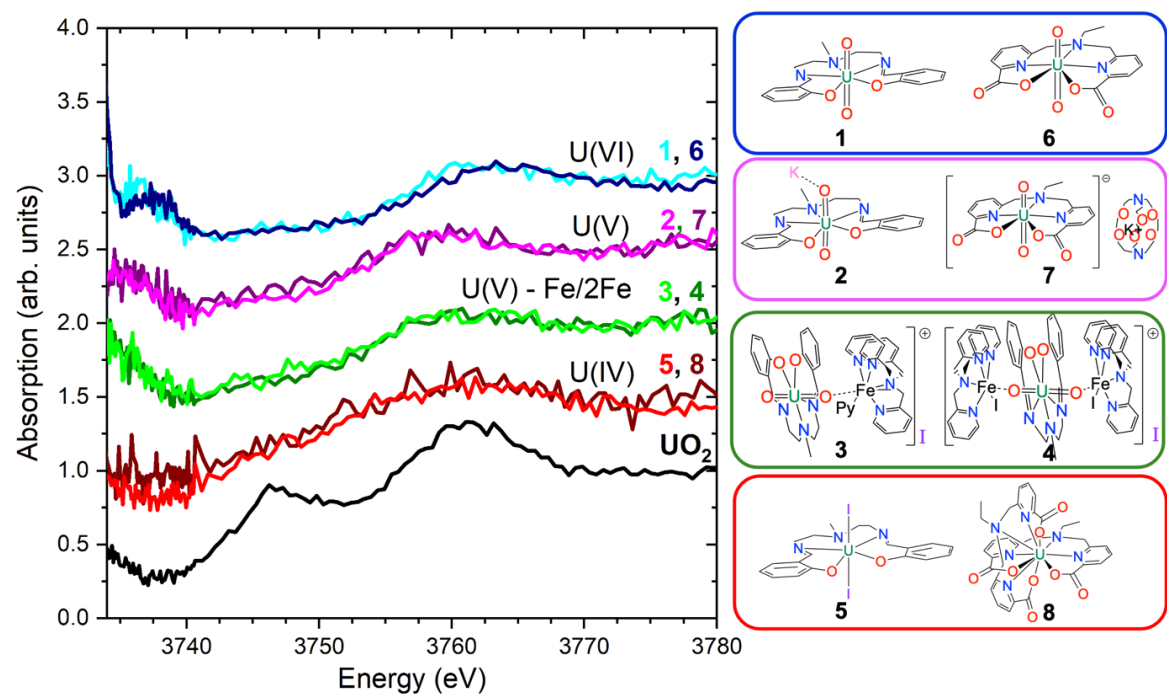


Figure S28. U M₄ edge HR-XANES (post edge region) of compounds 1 – 8.

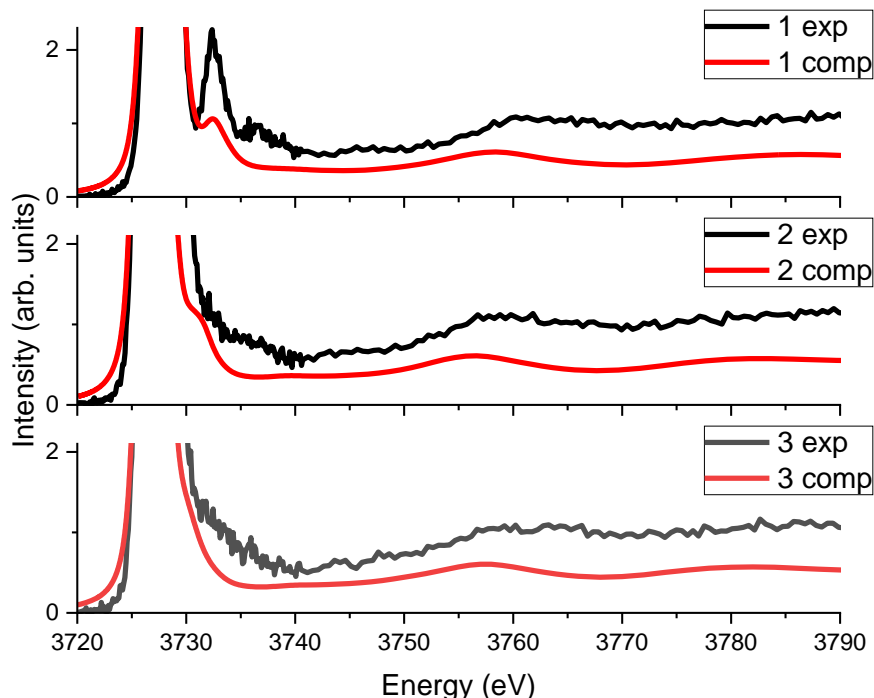


Figure S29. U M₄ edge HR-XANES post edge region of compounds 1 – 3.

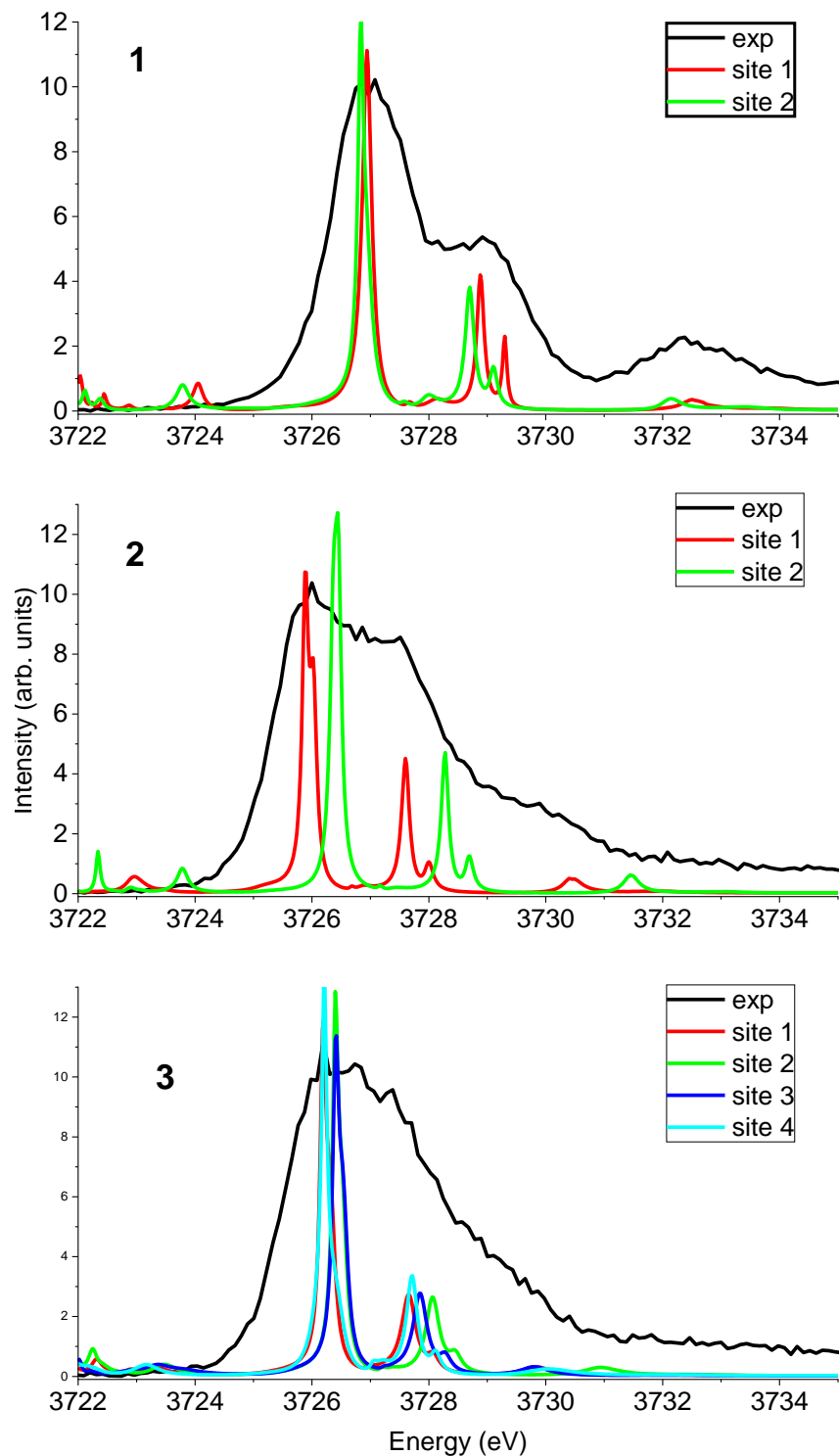


Figure S30. U M₄ edge HR-XANES of compounds 1 – 3 and spectra of the different U sites calculated by FDMNES.

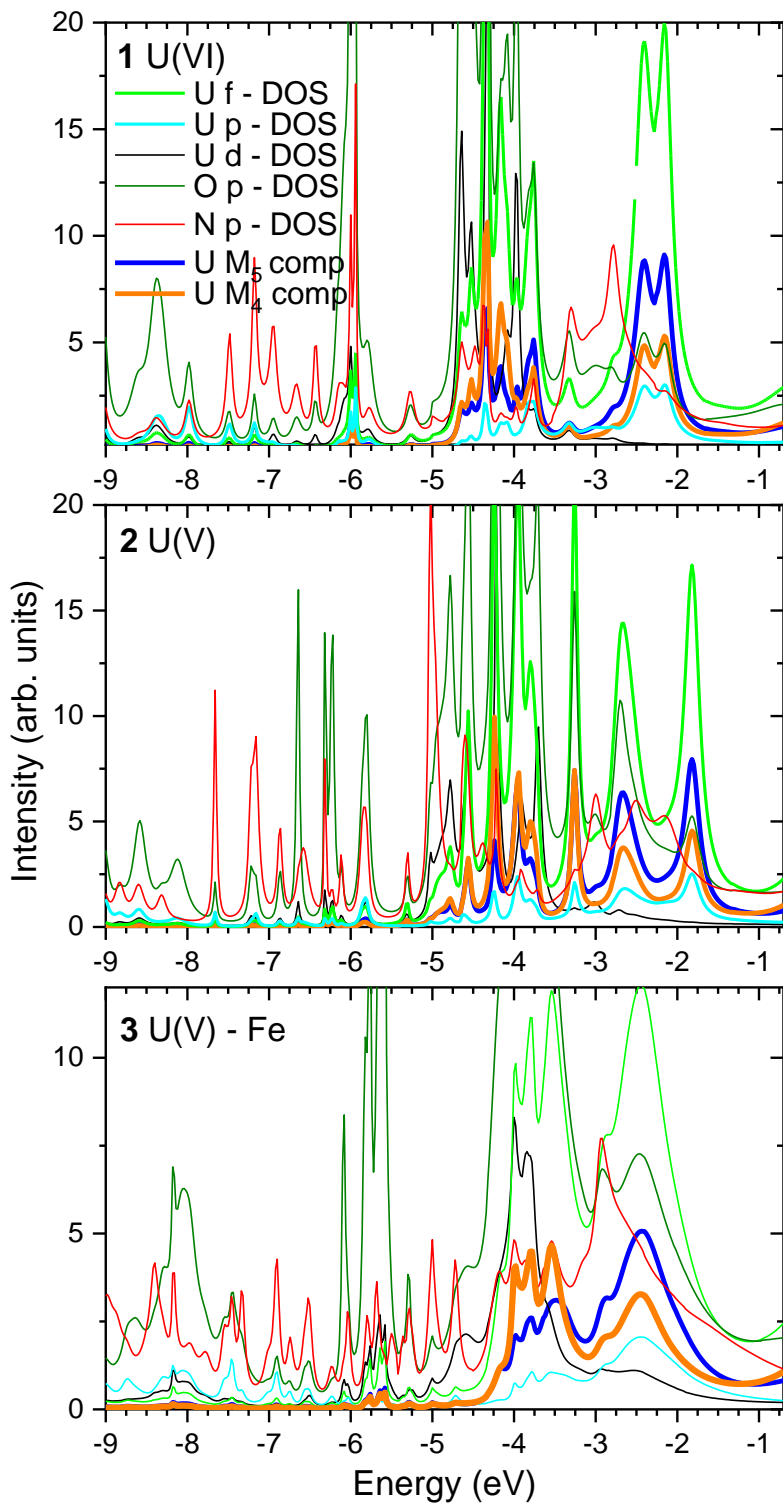


Figure S31. Occupied U p, d, f – DOS, O p – DOS and N p – DOS as well as XES spectra considering the selection rules for the U M₄ and U M₅ absorption edges.

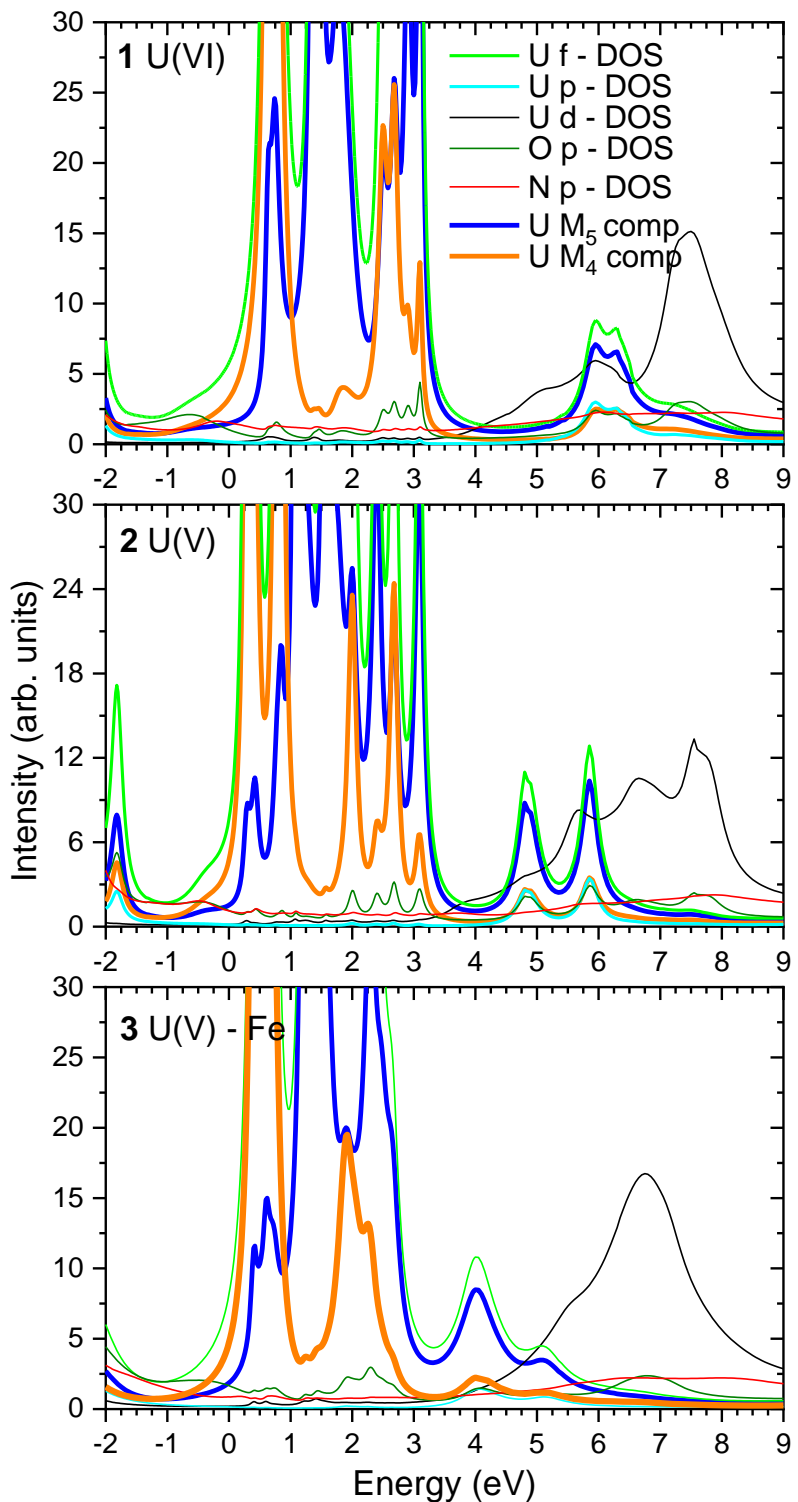


Figure S32. Occupied U p, d, f – DOS, O p – DOS and N p – DOS as well as HR-XANES spectra considering the selection rules for the U M₄ and U M₅ absorption edges.

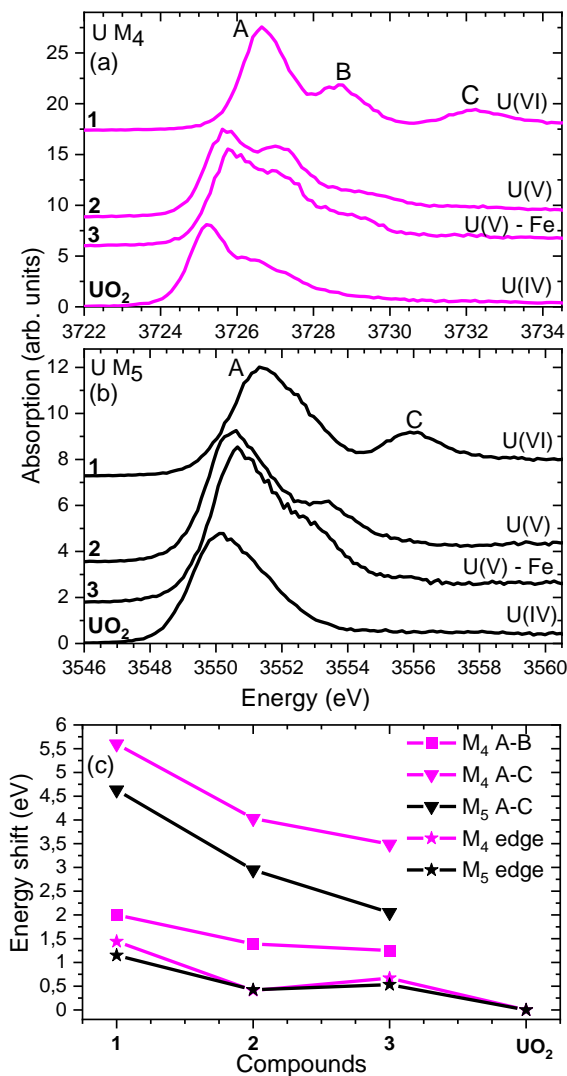


Figure S33. (a) The U M₄ and (b) M₅ edge HR-XANES spectra of 1, 2 and 3 compounds and the UO₂ reference. (c) Energy shifts between A, B and A, C spectral peaks as well as the relative energy shifts of the M₄ and M₅ absorption edges compared to the spectrum of UO₂.

Example FDMNES input file

```

Filout
  U(VI)/04/U(VI)
Range
  -30 0.02 4 0.05 10 0.2 15 1 40 2 70
Edge
  M4
Radius
  3.5
Quadrupole
SCF

```

```
Relativiste
Spinorbite
state_all
Z_absorber
    92
Cif_file
    U(VI)/U(VI).cif
End
```

References

1. Mazzanti, M., Natrajan, L., Burdet, F. & Pécaut, J. Synthesis and Structure of a Stable Pentavalent-Uranyl Coordination Polymer. *J. Am. Chem. Soc.* **128**, 7152–7153 (2006).
2. Monreal, M. J. *et al.* UI₄ (1,4-dioxane)₂, [UCI₄ (1,4-dioxane)]₂, and UI₃ (1,4-dioxane)_{1.5}: Stable and Versatile Starting Materials for Low- and High-Valent Uranium Chemistry. *Organometallics* **30**, 2031–2038 (2011).
3. Mougel, V., Pecaut, J. & Mazzanti, M. New polynuclear U(IV)-U(V) complexes from U(IV) mediated uranyl(V) disproportionation. *Chem. Commun.* **48**, 868–870 (2012).
4. Thapper, A. *et al.* Synthesis and characterization of molybdenum oxo complexes of two tripodal ligands: reactivity studies of a functional model for molybdenum oxotransferases. *Dalton Transactions* **0**, 3566–3571 (2005).
5. Pellissier, A. *et al.* Relating Structural and Thermodynamic Effects of the Pb(II) Lone Pair: A New Picolinate Ligand Designed to Accommodate the Pb(II) Lone Pair Leads to High Stability and Selectivity. *Inorg. Chem.* **46**, 3714–3725 (2007).
6. Chatelain, L., Pécaut, J., Tuna, F. & Mazzanti, M. Heterometallic Fe²⁺-UV and Ni²⁺-UV Exchange-Coupled Single-Molecule Magnets: Effect of the 3 d Ion on the Magnetic Properties. *Chem. Eur. J.* **21**, 18038–18042 (2015).
7. Faizova, R., Scopelliti, R., Chauvin, A.-S. & Mazzanti, M. Synthesis and Characterization of a Water Stable Uranyl(V) Complex. *J. Am. Chem. Soc.* **140**, 13554–13557 (2018).
8. CrysAlisPro Software System, Rigaku Oxford Diffraction, 2020.
9. Sheldrick, G.M., ShelXT-Integrated space-group and crystal-structure determination, *Acta Cryst. A* **71**, 3–8 (2015).
10. Sheldrick, G.M., Crystal structure refinement with ShelXL, *Acta Cryst.*, 2015, C71, 3–8.
11. Rothe, J., *et al.* Fifteen years of radionuclide research at the KIT synchrotron source in the context of the nuclear waste disposal safety case. *Geosciences (Switzerland)* **9**(2), 1–22 (2019).
12. Ravel, B.; Newville, M. ATHENA, ARTEMIS, HEPHAESTUS: data analysis for X-ray absorption spectroscopy using IFEFFIT. *J. Synchrotron Radiat.* **12**(4), 537–541 (2005).

